6-2020

FABRICATION, CHARACTERIZATION AND APPLICATIONS OF CHEMICALLY MODIFIED PLANAR METALLIC ELECTRODES FROM COPPER CLAD SHEETS

Rana T. K. Alsaidi

United Arab Emirates University

College of Science

Department of Chemistry

FABRICATION, CHARACTERIZATION AND APPLICATIONS OF CHEMICALLY MODIFIED PLANAR METALLIC ELECTRODES FROM COPPER CLAD SHEETS

Rana T. K. Alsaidi

This thesis is submitted in partial fulfilment of the requirements for the degree of Master of Science in Chemistry

Under the Supervision of Professor Sayed A. Marzouk

June 2020

Declaration of Original Work

I, Rana T.K. Alsaidi, the undersigned, a graduate student at the United Arab Emirates University (UAEU), and the author of this thesis entitled "*Fabrication, Characterization and Applications of Chemically Modified Planar Metallic Electrodes from Copper Clad Sheets*", hereby, solemnly declare that this thesis is my own original research work that has been done and prepared by me under the supervision of Professor Sayed A. Marzouk, in the College of Science at UAEU. This work has not previously been presented or published, or formed the basis for the award of any academic degree, diploma or a similar title at this or any other university. Any materials borrowed from other sources (whether published or unpublished) and relied upon or included in my thesis have been properly cited and acknowledged in accordance with appropriate academic conventions. I further declare that there is no potential conflict of interest with respect to the research, data collection, authorship, presentation and/or publication of this thesis.

Student's Signature: __Rana T. K. Alsaidi_____   Date: July 27, 2020

Advisory Committee

1) Advisor: Sayed A. Marzouk

Title: Professor

Department of Chemistry

College of Science

2) Co-advisor: Ahmed. S. Alshamsi

Title: Assistant Professor

Department of Chemistry

College of Science

3) Co-advisor: Muna S. Bufaroosha

Title: Associate Professor

Department of Chemistry

College of Science

Approval of the Master Thesis

This Master Thesis is approved by the following Examining Committee Members:

1) Advisor (Committee Chair): Sayed A. Marzouk

   Title: Professor

   Department of Chemistry

   College of Science

   Signature *Sayed Marzouk*　　　　　　　Date　6/8/2020

2) Member: Alaa Eldin Salem

   Title: Professor

   Department of Chemistry

   College of Science

   Signature　　　　　　　　　　　　　Date　6 / 8 / 2020

3) Member (External Examiner): Nathir Al-Rawashdeh

   Title: Professor

   Faculty of Engineering

   Institution: Higher Colleges of Technology/ RAS Al-Khaimah Women's Campus, United Arab Emirates.

   Signature　　　　　　　　　　　　　Date　6/8/2020

This Master Thesis is accepted by:

Acting dean of the College of Science: Professor Maamar Benkraouda

Signature ___*Maamar Benkraouda*___   Date _14 Sept. 2020_

Dean of the College of Graduate Studies: Professor Ali Al-Marzouqi

Signature _____   Date _14/9/2020_

Copy ____ of ____

Abstract

In this work, we developed a fabricating method for planar electrodes by milling and cutting copper clad sheets. The main objectives of this thesis are to produce customized planar electrodes with different geometries with relatively higher reusability compared to the screen-printed electrodes available by commercial vendors. The fabricated electrodes from copper clad sheets were electroplated with different metals using commercial electroplating baths to produce different metallic planar electrodes. Also, the fabrication of planar electrodes with cavities to be filled with modified carbon paste was done. The electroplated planar electrodes were characterized by cyclic voltammetry technique. In addition to that, they were applied to detect hydrogen peroxide (H_2O_2) amperometrically in the flow injection analysis mode. A preliminary experiment was also done to detect glycerol amperometrically using flow injection analysis mode by using copper as the working electrode. The result of the cyclic voltammetry experiments showed that the plated metallic layers exhibit close electrochemical behavior to their counterpart bulk metallic electrodes. The calculated detection limit for the H_2O_2 was found to be 38.4 µM and 48.5 µM for two different shapes of planar electrodes; the first planar electrode has a circular-shaped working electrode and the second planar electrode has a rectangular-shaped working electrode. The electrodes used were able to detect glycerol in the range 10 ppm to 160 ppm in alkaline medium. The described fabrication technique proved suitable to produce planar electrodes of much-enhanced reusability than the screen-printed electrodes and of comparable electrochemical performance to the bulk solid electrodes at a dramatically lower cost. The enhanced reusability is due to their ability to withstand harsh mechanical polishing with sandpapers then re-electroplate their surfaces again.

Keywords: Screen-printed electrodes, planar electrodes, electroplating, copper, gold, silver, nickel, platinum, cyclic voltammetry, amperometry, flow injection analysis, hydrogen peroxide (H_2O_2), glycerol.

Title and Abstract (in Arabic)

تصنيع، وتوصيف، وتطبيق أقطاب معدلة كيميائياً معدنية مستوية من ألواح النحاس المغطاة

الملخص

تختص هذه الرسالة بتطوير طريقة لتصنيع أقطاب مستوية عن طريق حفر وقطع صفائح النحاس المغطاة باستخدام ماكينات السي إن سي. الأهداف الرئيسية لهذه الأطروحة هي إنتاج أقطاب مستوية مخصصة بأشكال هندسية مختلفة مع إمكانية إعادة استخدام أعلى نسبيًا مقارنة بأقطاب الشرائح المطبوعة المتاحة من قبل الشركات المصنعة. تم طلاء الأقطاب المصنعة بمعادن مختلفة تشمل: النيكل، والفضة، والذهب، والبلاتين وذلك باستخدام حمامات الطلاء الكهربائي المتاحة تجارياً لإنتاج أقطاب معدنية مستوية مختلفة. كما أنه، تم تصنيع أقطاب مستوية مع تجاويف ليتم ملؤها بعجينة الكربون المعدل بمواد نشطة كهربائياً. تم توصيف الأقطاب المستوية المطلية كهربائياً بتقنية قياس الجهد الدوري. بالإضافة إلى ذلك تم استخدامها للكشف عن فوق أكسيد الهيدروجين (H_2O_2) والجليسرين بتقنية الأمبيرومتري باستعمال طريقة تحليل الحقن المستمر. أظهرت نتائج تجارب قياس الجهد الدوري أن الطبقات المعدنية المطلية تظهر سلوكًا كهروكيميائياً قريبًا من الأقطاب المعدنية الصلبة المناظرة لها. هذا ووجد أن حد الكشف المحسوب لـ H_2O_2 هو 38.4 و48.5 ميكرومول ليتر$^{-1}$ لشكلين مختلفين من الأقطاب المستوية التي تم استخدامها في هذه الدراسة. كانت الأقطاب المستخدمة قادرة على كشف الجليسرين في نطاق 10 - 160 جزء في المليون في الوسط القلوي. إن طريقة التصنيع الموصوفة قادرة على إنتاج أقطاب مستوية يمكن استعمالها بدلاً من أقطاب الشرائح المطبوعة مع إمكانية إعادة استخدام بشكل محسن وأداء كهروكيميائي مماثل للأقطاب الصلبة بتكلفة أقل بشكلٍ كبير. إن إعادة الاستخدام المحسنة ترجع إلى قدرتها على تحمل الصقل الميكانيكي القاسي بورق الصقل ثم إعادة طلاء أسطحها كهربائياً مرة أخرى.

مفاهيم البحث الرئيسية: الأقطاب الشريحية المطبوعة، الأقطاب المستوية، الطلاء كهربائي، نحاس، ذهب، فضة، نيكل، بلاتين، قياس الجهد الدوري، التحليل الأمبيرومتري، تحليل الحقن المستمر، فوق أكسيد الهيدروجين (H_2O_2)، الجليسرين.

Acknowledgments

I wish to express my deepest gratitude to my advisor Prof. Sayed A. Marzouk for his guidance and supervision. Also, I would like to extend my gratitude to my co-advisors Dr. Ahmed. S. Alshamsi and Dr. Muna S. Bufaroosha for their continued support during this study.

I would like to thank the chair of the Department of Chemistry Dr. Mohamed Alazab Alnaqbi, the Master of Science in Chemistry program coordinator Prof. Thies Thimann and previously Prof. Abbas Khalil for their assistance and guidance during my study at UAEU.

My warmest gratitude goes to my parents, brother, and sisters for their support, unending encouragement, and motivation throughout my study and during writing my master thesis.

Dedication

To my beloved parents and family.

Table of Contents

List of Tables

List of Figures

List of Abbreviations

CE	Counter electrode
CNC	Computer numerical control
CV	Cyclic voltammetry
EIV	Electronic injection valve
FIA	Flow injection analysis
FR	Flow rate
GCE	Glassy carbon electrode
LOD	Limit of detection
LOQ	Limit of quantitation
PCB	Printed circuit board
PEDOT	Poly(3,4-ethylenedioxythiophene)
PESOT-PS	Poly(3,4-ethylenedioxythiophene) polystyrene sulfonate
RE	Reference electrode
RPM	Revolution per minute
SPEs	Screen printed electrodes
WE	Working electrode
WHO	World Health Organization

Chapter 1: Introduction

1.1 Overview

Screen-printed electrodes are small electrodes employed in different applications, cheap, and disposable. It is a tool that is widely used to detect different analytes (Taleat, Khoshroo, & Mazloum-Ardakani, 2014). Students use them to learn the essential concepts in electrochemistry (Chyan & Chyan, 2008). Screen-printed electrodes come in a variety of shapes, geometries, and sizes. Normally, a base substrate made of plastic, ceramic, paper, or glass is used to print on the electrode(s) using screen-printing technology (Antuña-Jiménez, González-García, Hernández-Santos, & Fanjul-Bolado, 2020). An example of a screen-printed electrode is shown in Figure 1.
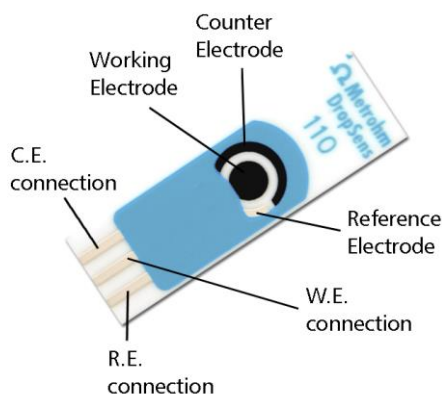
Figure 1: Screen-printed electrode. From *Metrohm DropSens.* Retrieved from http://www.dropsens.com/en/screen_printed_electrodes_pag.html. Copyright 2020 by DropSens.

Screen-printed electrodes offer their users the ability to produce and modify the electrodes with new novel ideas that serve their research, and educational targets with a large space of creativity. The sensitivity and the selectivity of screen-printed electrodes can be improved by changing the type of the ink used to print the electrodes, making some delicate mechanical polishing (Cumba et al., 2016), doing some electrochemical pretreatment (Su, Wang, & Cheng, 2011); or by modifying their surfaces with nanoparticles, metal-organic framework-based hybrid materials (Ezhil Vilian et al., 2017), or enzymes (Ledru, Ruillé, & Boujtita, 2006), etc.

Screen-printed electrodes have been used as the platform for many sensing devices (Antuña-Jiménez et al., 2020). The majority of blood glucose sensors are categorized as amperometric sensors (Zhang & Hoshino, 2013). A report was published in the "Diabetes Technology & Therapeutics" journal in 2009, pointed out that the self-measurement of blood glucose has become a multi-billion dollar industry (McGarraugh, 2009). According to the World Health Organization (WHO), 2.2 million deaths were due to high blood glucose in 2012. While in 2016, diabetes was the direct cause of 1.6 million deaths (World Health Organization, 2020). This shows how important it is to invest in developing sensors platforms like screen-printed electrodes.

1.2 Statement of the Problem

With all the advantages that screen-printed electrodes provide, they pose some limitations such as the limited reusability due to their disposable nature, and the customized geometries from commercial vendors add additional high cost to the users. So, in this work, we describe a method of fabrication planar electrodes with the goals of (i) providing an alternative cheaper method to fabricate customized planar electrodes (ii) fabricating different new geometries of planar electrodes, including

planar electrodes with cavities to be filled with carbon paste; to open the door for the planar chemically modified carbon electrodes and (iii) producing planar electrodes with enhanced reusability compared to screen-printed electrodes and comparable to solid electrodes.

The proposed fabrication method includes the use of the available CNC machine with its software to design, cut, and mill different planar electrodes with different designs. Copper clad sheets were chosen to be the substrate for these electrodes for two main reasons. Firstly, copper has the second-highest electrical conductivity between metals after silver (West, 1974 as cited in Walsh, 1991; Kaye & Laby, 1989 as cited in Walsh, 1991; Ellis, 1984, as cited in Walsh, 1991). Secondly, the relatively low cost of copper compared to silver. The obtained electrodes will be plated with different metals using commercially available electroplating baths to produce different metallic finishing layer i.e. nickel, gold, silver, and platinum. Also, planar electrodes with some cavities will be made to fill them with modified carbon pastes. The resulting electrodes will be characterized using cyclic voltammetry technique. In addition to that, they will be used in different flow injection analysis experiments to study their behavior.

1.3 Relevant Literature

Due to the huge importance of electrodes in electrochemistry, a brief review of electrodes, their types, and applications is presented with emphasis on screen-printed electrodes.

1.3.1 Background

Electrochemistry has been defined as the branch of chemistry that deals with the interrelation between electrical and chemical effects (Bard & Faulkner, 2000). It covers a wide array of applications like batteries, electroanalytical sensors, and electrochromic displays. Various phenomena like electrophoresis and corrosion as well as technologies like the large-scale production of chlorine and aluminum and metals electroplating are based on electrochemistry (Bard & Faulkner, 2000).

Electroanalytical chemistry concerns with methods of measuring electrochemical phenomena and their applications to chemical analysis (Izutsu, 2002). The first analytical application of electrochemistry was reported in 1801 by Cruikshank, who electrolyzed solutions of copper and silver salts and suggested that the electrolytic deposits could be used as a means of identifying those metals. Thenceforth, different electrochemical techniques have been evolved (Izutsu, 2002).

Electroanalytical methods are classified based on the place of the reaction (relative to the electrode) into interfacial methods and bulk methods (Skoog, Holler, & Crouch, 2007). In the interfacial method, electrochemical reactions occur at the interface between the electrode surfaces and the thin layer of the solution near to it. Interfacial methods are subdivided into static methods where there is no current in the electrochemical cell and dynamic methods where there is current in the electrochemical cell. The static method includes potentiometry and potentiometric titrations. While the dynamic methods include a wide variety of methods that either controlled potential methods or methods with a constant current. In controlled potential methods, the potential of the cell is controlled while measuring other variables. Examples of these methods are electrogravimetry, amperometric titrations,

voltammetry, and constant electrode potential coulometry. In the constant current dynamic methods, there is a current in the electrochemical cell but that current is held constant while collecting the data. These methods include coulometric titrations and electrogravimetry. On the other hand, the bulk methods group contains conductometry and conductometric titrations (Skoog et al., 2007). Figure 2 presents this classification.
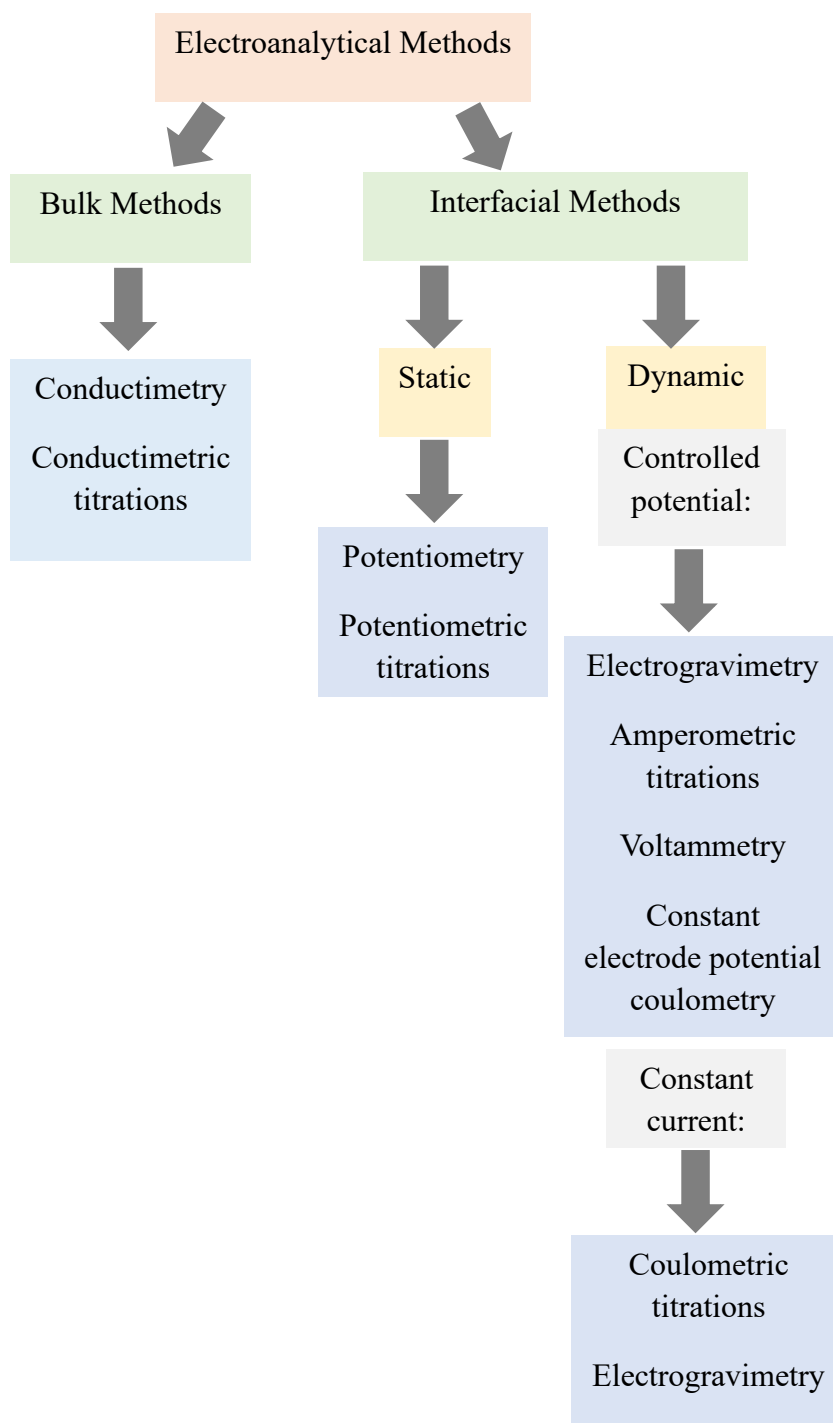
Figure 2: Electroanalytical methods classification based on the place of the reaction relative to the electrode.

Another classification that is based on the electrode reactions was also reported (Izutsu, 2002). Methods based on electrode reactions were subdivided into three subgroups. The first subgroup includes methods that completely electrolyze the species under investigation these include electrogravimetry and coulometry. The second subgroup includes methods that partially electrolyze the electroactive species under investigation these include direct current polarography/voltammetry, alternating current polarography/voltammetry, squarewave polarography/voltammetry, pulse methods for polarography and voltammetry, amperometry, chronopotentiometry, and polarography and voltammetry at the interface between two immiscible electrolyte solutions. The third subgroup includes methods that do not electrolyze the electroactive species under investigation these include potentiometry and tensammetry (Izutsu, 2002). On the other hand, methods that are not based on electrode reactions include conductimetry and high frequency methods (Izutsu, 2002). Figure 3 shows this classification.
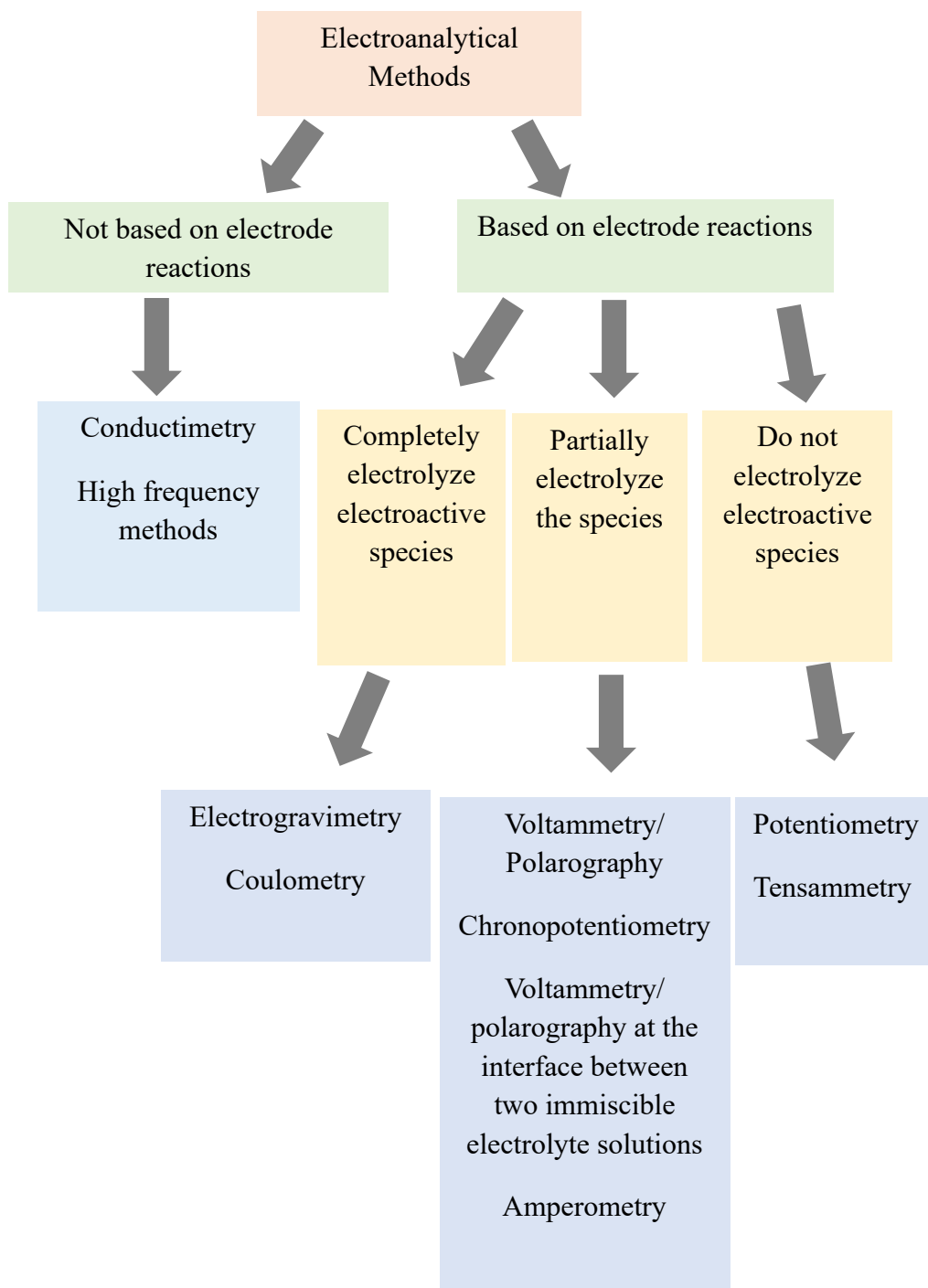
Figure 3: Electroanalytical methods classification based on electrode reactions.

So, from the discussion above it is quite apparent that all electroanalytical methods need an electrode of a certain type. The following sections will be devoted to the different types of electrodes and their applications with emphasis on screen-printed electrodes.

1.3.2 Electrodes

Electrodes are made from various materials that include solid and liquid metals, carbon, and semiconductors (Bard & Faulkner, 2000). Solid metals like platinum and gold. Liquid metal like mercury and amalgam. Carbon electrodes can be graphite, glassy carbon, or boron-doped diamond. Semiconductors are like indium-tin-oxide, or silicon (Bard & Faulkner, 2000). There are many properties that a solid material must have to function as an electrochemical electrode. These include (i) reproducibility in the physical, chemical, and electronic properties, ii) to be hard and durable, iii) can be easily manufactured, iv) of low cost, v) exhibit rapid electron-transfer kinetics for a wide array of redox systems, (vi) exhibit a stable and homogeneous morphology and microstructure over a wide potential range, (vii) poses good chemical inertness, (viii) characterized with high electrical conductivity, and (ix) exhibit low background current (Swain, 2007).

1.3.3 Types of Electrodes

Different types of electrodes are available for research and analytical applications. Some of the available types of electrodes including microelectrodes, solid electrodes, screen-printed electrodes, and copper-clad boards, and printed circuit boards electrodes are reviewed in the following sections.

1.3.3.1 Microelectrodes

Microelectrodes describe electrodes that have dimensions in the micrometer or nanometer range (Bard & Faulkner, 2000). They describe electrodes in which when the current pass the solution through the electrode the current will not change the bulk concentration of electroactive species. This will happen when the area of the electrode (A) is small enough and the volume of the solution (v) is large enough. This condition is known as small A/v (Laitinen & Kolthoff, 1939; Bard & Faulkner, 2000).

Microelectrodes have many advantages. They provide a relatively easy way to measure very small currents as low as 10^{-17} A. The iR losses limited the electrochemical experiments done with large electrodes to ionically conducting solutions. However, minimized iR losses in the solution is achieved with microelectrodes due to their small size. Moreover, their sufficiently small sizes reduce the capacitive current. In addition to that, the rate of mass transport at the electrode increases as its size gets smaller so the steady states of mass transfer are reached quickly. Microelectrodes also show excellent signal to noise ratios (S/N) due to the decreased capacitive current and the increased rates of mass transport. In addition to that, microelectrodes systems are relatively cheap and employed easily (Fleischmann & Pons, 1987).

Some of the microelectrodes disadvantages include the difficulties in doing reproducible polishing, maintaining a clean electrode's surface, surface fouling in real industrial or environmental samples, and the noise that results from electrode imperfections (Bond, 1994).

Microelectrodes are used in diverse areas. For example, in applications where the solution is not highly ionic conducting one and when small electrodes are needed

(Foster & Keyes, 2006). For instance, ruthenium purple modified carbon fiber microelectrodes were made to detect hydrogen peroxide in brain tissue (Ledo, Fernandes, Brett, & Barbosa, 2020). Also, in applications where one needs to get an insight into redox processes that occur on short timescales (microsecond and nanosecond) (Foster & Keyes, 2006).

Many works were reported on microelectrodes. pH microelectrode based on nanostructured palladium hydride was reported (Serrapede, Pesce, Ball, & Denuault, 2014). The potentiometric response of this microelectrode was found to be Nernstian from pH 1 to pH 14 (Serrapede et al., 2014). A needle-type microelectrode array sensor based on gold electrode was developed for in situ measurements of dissolved oxygen (Lee, Lim, Seo, Bishop, & Papautsky, 2007). The sensitivity achieved with this sensor was ~200 pA/ mg L in oxygenated saline solution and ~147 pA/ mg L in an oxygenated mineral salt solution (Lee et al., 2007).

1.3.3.2 Solid Electrodes

Solid electrodes come in many different shapes. They could be in a form of wires e.g. silver or platinum wires (Dobčnik, Gros, & Kolar, 1998; Lingane & Lingane, 1963). They could be in a form of metallic rods (Martins, Nunes, Koch, Martins, & Bazzaoui, 2007), or the wire may be encapsulated with an insulation material leaving only a cross-sectional area of the wire (Neelakantan & Hassel, 2007). The applications vary a lot. For instance, a modified gold wire with gold nanoparticles followed by acetylcholinesterase enzyme was applied to detect acetylcholinesterase inhibitors (Shulga & Kirchhoff, 2007). Also, a nickel rod was used to detect glucose nonenzymatically using flow injection analysis (Zhao, Shao, Li, & Jiao, 2007).

1.3.3.3 Screen-printed Electrodes

Screen-printed electrodes are produced by printing different inks on substrates made of plastic or ceramic (Renedo, Alonso-Lomillo, & Martínez, 2007). The type of ink used determines the selectivity and sensitivity of the electrode (Renedo et al., 2007). The substrate could be made of polycarbonate, polyimide, and polyether ether ketone (Fletcher, 2016). However, polyesters substrates are one of the common substrates used in the screen-printed electrode (Renedo et al., 2007).

Screen-printed electrodes are available from different suppliers which offer a wide range of choices for the consumer like Metrohm DropSens (http://www.dropsens.com/en/screen_printed_electrodes_pag.html) and Zimmer and Peacock (https://www.zimmerpeacocktech.com/products/unmodified-sensors/). Fletcher (2016) pointed out that the screen-printing process provides many advantages for electrodes fabrication. The three main advantages of screen-printing method over other electrode's fabrication methods include: i) the ease of control of the electrode area, thickness, and composition, ii) the possibility of doing statistical validation for experimental results due to the existence of replicate electrodes, iii) the ability to add catalysts to the ink easily (Fletcher, 2016).

In the following subsections, the different types of screen-printed electrodes are reviewed briefly.

1.3.3.3.1 Screen-printed Carbon Electrodes

Screen-printed carbon electrodes constitute an important type of screen-printed electrodes, this has been discussed in detail by Fletcher in (Fletcher, 2016). Carbon black and activated carbon are the most widely used forms of carbon. Other interesting types include carbon nanotubes, carbon nanofibers, and graphene (Fletcher, 2016).

Fletcher (2016) also discussed the essential components of the ink and its properties. The components of the ink include i) conducting filler, ii) volatile solvent, iii) and non-conducting binder. The volatile solvent will dry after printing is done leaving behind the conducting filler and the non-conducting binder in a process known as curing. The conducting filler will be attached to the non-conducting binder. In some cases, there will be a contamination from the residuals of the non-volatile solvent that were not evaporated. So, it is important to ensure that the volatile solvent used is electrochemically inactive over a wide range of potentials. This characteristic of the solvent can also be referred to as the "electrochemical stability window". In addition to that, the solvent must be free from non-volatile impurities. Toxicity is also an important factor that one should look at when choosing the volatile solvent (Fletcher, 2016).

Several applications using screen-printed carbon electrodes have been reported. Krejčí and coworkers (2004), used graphite screen-printed electrode to detect hydrogen peroxide at +0.65 V (Krejčí et al., 2004). Bergamini and coauthors (2007) used a carbon ink screen-printed electrode to determine procaine (which is a short-acting ester-linked local anesthetic (Weinschenk et al., 2017)) in pharmaceutical formulation at +0.80 V (Bergamini, Santos, Stradiotto, & Zanoni, 2007). Honeychurch and coworkers (2002), used screen-printed carbon for the determination of Cu^{2+} at trace levels using differential pulse anodic stripping voltammetry. They studied the effect of Bi^{3+}, Cd^{2+}, Fe^{3+}, Hg_2^{2+}, Pb^{2+}, Sb^{3+}, and Zn^{2+} on the Cu stripping peak. Under the conditions employed in their study, only Hg_2^{2+} was found to significantly affect the response (Honeychurch, Hawkins, Hart, & Cowell, 2002).

1.3.3.3.2 Screen-printed Metal Electrodes

Screen-printed metal electrodes are another important category of screen-printed electrodes. Electrodes made with different metals, e.g., gold, platinum, silver, and palladium are available in the market by commercial vendors like Metrohm DropSens (http://www.dropsens.com/en/screen_printed_electrodes_pag.html). In addition to that, they have been produced in research laboratories (Metters, Tan, Kadara, & Banks, 2012). Screen-printed metal electrodes have been used in many applications. For example, tetracycline residues in food were determined by a gold screen-printed electrode (Masawat & Slater, 2007). The detection of trace lead was also done using a gold screen-printed electrode (Laschi, Palchetti, & Mascini, 2006). Hydrazine and hydrogen peroxide were detected using a platinum screen-printed electrode (Metters et al., 2012). Sophocleous and Atkinson (2017) made a whole review concerning about the screen-printed silver/silver chloride reference electrodes (Sophocleous & Atkinson, 2017).

1.3.3.3.3 Miscellaneous Types of Screen-printed Electrodes

There are many types other than carbon screen-printed electrodes and metals screen-printed electrodes in which in this literature review are grouped under the "Miscellaneous types of screen-printed electrodes" section. For example, modified metal screen-printed electrode like gold and platinum screen-printed electrodes modified with Prussian Blue was used for the amperometric detection of hydrogen peroxide (de Mattos, Gorton, & Ruzgas, 2003). Bismuth oxide screen-printed electrode was used for voltammetric trace screening of lead (II), cadmium (II), and zinc (II) (Kadara, Jenkinson, & Banks, 2009). Other available screen-printed electrodes commercially available by Metrohm DropSens

(http://www.dropsens.com/en/screen_printed_electrodes_pag.html) include the optically transparent indium tin oxide screen-printed electrodes, the [poly(3,4-ethylenedioxythiophene)] (PEDOT) screen-printed electrode, and the thick-film electrodes made of bismuth, antimony, chromium, nickel, tin, aluminum, molybdenum, lead, tantalum, tungsten, steel, carbon steel, and cobalt.

1.3.3.4 Copper Clad Boards and Printed Circuit Boards (PCB) Electrodes

Copper clad boards electrodes have been employed in the fabrication of electrodes. Electrodes made of copper clad boards modified with gold nanostructures in combination with poly(3,4-ethylenedioxythiophene) polystyrene sulfonate (PEDOT-PSS) were used for the detection of the potent carcinogen methylene blue dye in water (Gupta, Juneja, & Bhattacharya, 2020).

Electrodes based on printed circuit boards have been used in many applications. Dutta and coauthors (2018), fabricated glucose sensors based on printed circuit board electrodes in which they immobilized glucose oxidase covalently on a chemically pre-treated, gold plated working electrodes (Dutta, Regoutz, & Moschou, 2018). Printed circuit board electrode was also used to produce a biosensor to target carcinogenic embryonic antigen which is a cancer biomarker (Moreira, Ferreira, Puga, & Sales, 2016). Electrodes based on printed circuit boards are available by commercial vendors like Zimmer and peacock company (https://www.zimmerpeacocktech.com/products/biosensor-builders-kit/pcb-biosensor/).

Chapter 2: Experimental Work and Set-up

2.1 Reagents and Materials

Silver pen plating solution, gold tank replenisher, gold strike solution, nickel pen plating solution, nickel brush plating solution, gold tank plating solution, gold pen plating solution, were purchased from Spa Plating Ltd., UK. Gold finishing polish, nickel plating solution, silver plating solution, and gold plating solution, were purchased from Gold Solutions, UK. Platinum plating solution (PT4 platinum ready to use plating bath 4g/L) was purchased from Legor Group S.p.A., Italy. Nitric acid 65% (w/v) was received from Panreac, Spain. Sulfuric acid 96% (w/v) and hydrochloric acid (37% w/v) were received from Applichem Panreac ITW companies, USA. Sodium hydroxide was received from Sigma-Aldrich, Germany. Sodium phosphate monobasic and dibasic anhydrous were received from DAEJUNG, South Korea. Sandpapers from Saint-Gobain Abrasives/flexOvit, France, and from Gallery^{TM}. 50,000 grit and 200,000 grit diamond pastes from Tech Diamond Tools, California USA. EpoThin® epoxy (resin No. 20-8140-128, hardener No. 20-8142-064) from Buehler, USA. Glycerin USP from AMEYA FZE, U.A.E. Copper clad sheet made of 0.25-mm thick copper layer sandwiched between two FR-4 sheets each with 1 mm was ordered from UC GROUP LIMITED, China. All chemicals were used without further purification and all solutions were prepared using deionized water.

2.2 Equipment and Electrodes

Pen plating equipment and titanium coated with mixed metal oxides mesh electrodes were received from Spa Plating Ltd., England. Solid nickel electrode from amazon. Pt disc electrode -5 mm dia- was received from BAS, Japan. Gold disc

electrode -2 mm dia- was received from CHI, USA. Copper rod electrode was received from Alfa Aesar, Germany. Silver wire electrode (1/8" dia, 99.95%) was received from SurePure Chemicals L.L.C., New Jersey USA. pH/mV meter model 420A+ was received from Thermo Orion, USA. D-23 miniTron Desktop CNC Router machine from CanCam, Canada. Dremel® 4000 rotary polisher tool from Dremel, USA. Electric car polisher from amazon, Princeton Applied Research Scanning potentiostat Model 362 from AMETEK, Inc., Pennsylvania USA. EmStat2 potentiostat and EmStat3 blue potentiostat were purchased from Palmsens BV, The Netherlands. LC-20AD HPLC pump from Shimadzu Scientific Instruments, Columbia, Maryland USA. 6 ports electronic injector installed with a 100-µl sample loop were purchased from VICI Valco Instruments Co. Inc., Texas USA.

2.3 Planar Electrodes Manufacturing

Several steps were done to produce the planar electrodes having different designs and different metallic coatings as shown in the below sections.

2.3.1 Designing the Planar Electrodes

VCarve Pro software (version 9) was used to design the different patterns of the planner electrodes. The software generates the G-codes that were used by the CNC machine to mill and cut the substrates. An example of the designs made is shown in Figure 4. The length and the width of the total area of one strip were 3.4 cm x 1.0 cm (length x width). The details of the planar electrodes' geometries are as following:

A. A single oval electrode having an 8 mm length x 0.4 mm width on one strip.

B. A single oval electrode having a 12 mm length x 4 mm width on one strip.

C. Three linear adjacent electrodes consisting of reference, working, and counter electrodes on one strip

D. A disc working electrode (5 mm diameter) surrounded by a reference electrode and a counter electrode on one strip.

E. An electrode with three cavities in one strip (for modified planar carbon electrode).

F. A working electrode with one cavity in one strip (for modified planar carbon electrode).
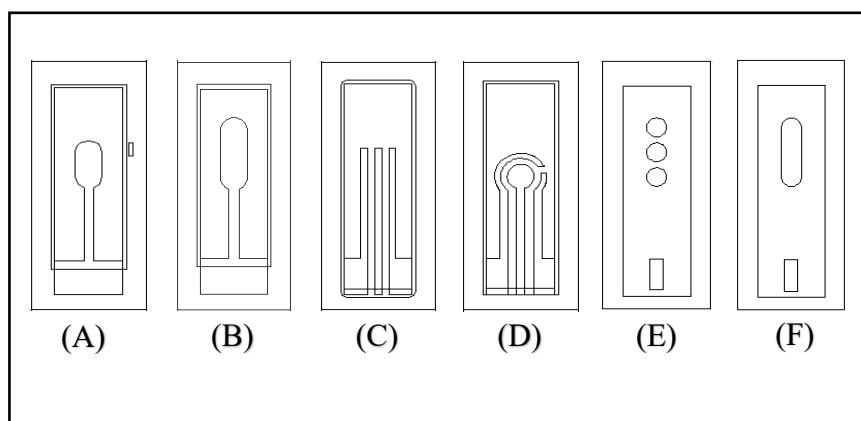
Figure 4: An example of the designs of the planar electrodes.

2.3.2 Milling and Cutting Electrode Substrates using the CNC Machine

The CNC machine was used to mill and cut the electrodes. The board consisted of a layer of a copper sheet with a thickness of 25 mm sandwiched between two FR-4 (a composite material made of glass fibers embedded in an epoxy resin (Djordjevic, Biljié, Likar-Smiljanic, & Sarkar, 2001)) each having a thickness of 1 mm. After cleaning the board area from the debris produced during the milling step, an epoxy layer was applied manually to the whole board area for all the designs except for electrodes E and F. After the epoxy was hardened, a facing step was done by generating

a G-code to the whole working area of the board. The purpose of the facing step was to minimize any differences in the thickness that occurred after adding the epoxy layer. However, during the facing step, the copper may be damaged due to variations in the thickness of the epoxy layer. To minimize the losses due to the facing step, the designs of the planar electrodes were placed sequentially raw by raw as shown in Figure 5. Then, another G-code was made to cut the strips into individual pieces. By using one board, 152 strips could be manufactured in case no damage occurred during the cutting and milling step.
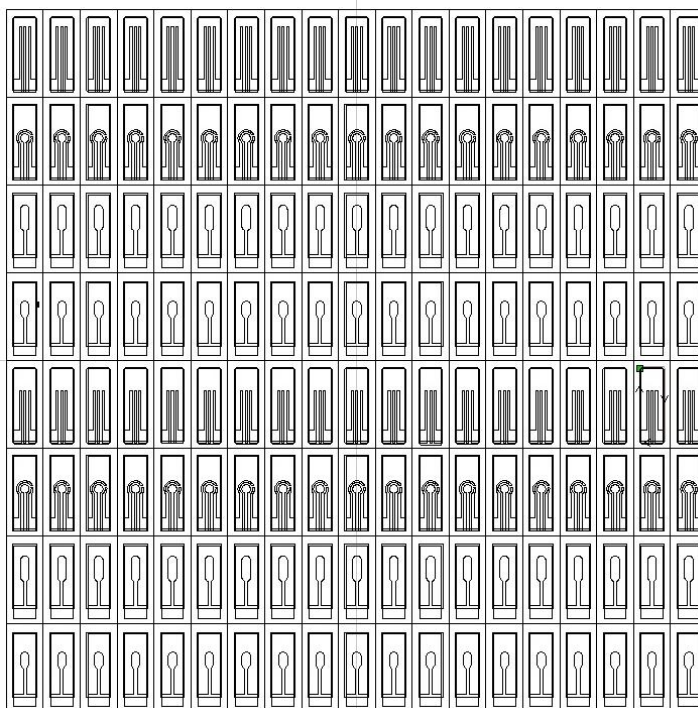

Figure 5: An example of the design of one board showing different planar electrodes designs.

2.3.3 Electroplating of the Electrodes using Commercial Electroplating Baths

Different commercial electroplating baths were used to plate the manufactured electrodes. Tank electroplating was used to plate the electrodes that were used for the characterization of the electrodes using the electroanalytical methods. Electrodes A and B were used for this purpose. While pen electroplating was used to plate the electrodes that were used in the flow injection analysis experiments. This was done using electrodes C and D. Tank electroplating was done using a two-electrodes cell configuration that utilizes a titanium coated with mixed metal oxides mesh working electrode as the anode and the desired planar electrode to be plated as the cathode. The required potential and/or current was adjusted using Princeton Applied Research Scanning potentiostat Model 362. Each time the cell was filled with a different electroplating tank to electroplate the electrodes with different metal while stirring the solution. Pen electroplating was done using the battery-powered plating pen from Spa Plating Ltd. In both types of electroplating, multiple layers of different metals were electroplated for more protection. Then, the final desired metallic layer was electroplated.

Depending on the state of the copper metal, sandpapers of progressively finer mesh were used to polish the electrode surface before the electroplating step was done. After polishing with sandpapers, the electrodes were rinsed with water. After that, 50,000 grit diamond paste then 200,000 grit diamond paste were applied on a tissue to polish the surface of the copper progressively. Subsequently, the electrodes were washed with detergent and rinsed thoroughly with distilled water unless otherwise stated.

2.4 Characterizing the Planner Electrodes using Electroanalytical Methods

After plating the electrodes with the different metallic layers electrochemically, cyclic voltammetry was used to characterize the plated layers. The cyclic voltammetry experiments were carried out using Em Stat2 potentiostat. A three-electrode cell was built for the electroanalytical characterization experiments. Namely, an Ag/AgCl reference electrode, a 5-mm diameter Pt counter electrode, and the electrochemically plated copper working electrode that is under investigation. Another set of cyclic voltammetry experiments were done for solid metallic electrodes using a three-electrode cell configuration that utilizes an Ag/AgCl reference electrode, a 5-mm diameter Pt counter electrode, and the solid metallic working electrode that is under investigation. Digital simulations of the voltammograms were performed with PS trace software (PalmSens) by using the scientific mode. The voltammograms were then plotted using OriginPro 2020 software.

2.5 Examining the Edge's Effect on the Behavior of the Electrochemical Plating

The edges' (boundaries between the copper and the epoxy) effect on plating was studied with two different working electrodes having two different shapes. The first working electrode was a copper rod electrode in which there was no epoxy applied to on it, thus no copper/epoxy boundaries present. It was plated using the plating pen equipment with Ni, Au, Ag, Au then Pt. After that, it was cycled in 0.5 M H_2SO_4. After recording the cyclic voltammogram the circumference of the copper rod electrode was covered by an insulator (a nail polish). In addition to that, a new layer of Au and then Pt were plated on it. Finally, a cyclic voltammogram was recorded again in 0.5 M H_2SO_4. The other electrode used to examine the edge effect was the planar electrode with (oval shape) in which the working electrode was plated in the same sequence

done on the copper rod electrode. The other steps were done in the same way done with the copper rod electrode as well.

2.6 Application of the Fabricated Electrodes in Flow Injection Analysis

Electrodes C and D were used to detect H_2O_2 by amperometry at +0.7 V. Different standard solutions 50, 100, 250, and 500 µM of H_2O_2 were freshly prepared in deionized water. 0.1 M Phosphate buffer saline pH (7.0) was used as a carrier solution for the H_2O_2 detection experiments. The flow rate effect on the electrodes' response was studied by constructing calibration curves at a flow rate of 0.5 ml/min, 1.0 ml/min, and 1.5 ml/min. The stability of the electrode response was also studied using a series of injections of 100 µM H_2O_2 at +0.7 V at 1.0 ml/min flow rate. A hair developer sample was purchased from a local market in Al Ain, U.A.E. (made in France) to determine its H_2O_2 content. The hair developer sample was stored in the fridge at $-4°C$ when not in use. Freshly before the flow injection analysis experiments, the hair developer sample was diluted by a factor of 5000 using deionized water. For electrode D a calibration curve was established again at 1.0 ml/min flow rate before injecting the diluted sample since it was injected on a different day than the day where the flow rate effect experiments were conducted. The final plated layer on the working, counter, and reference electrode were platinum, platinum, and silver, respectively.

In addition to that, a preliminary experiment for the amperometric detection of glycerol was carried out using type C and D electrodes. The procedure was as reported in the literature with some modifications (Maruta & Paixão, 2012). So, different standard solutions 10, 20, 40, 80, 160 ppm of glycerol were prepared in deionized water. 2 M NaOH was used as the carrier solution with 1.0 ml/min flow rate. The applied potential was +0.65 V. The as produced plain copper (without any electroplating) was used as the working

electrode while the final plated layer on the counter and reference electrode were platinum and silver, respectively.

The potential in the flow injection analysis experiments was controlled using EmStat3 blue potentiostat. And the digital simulations of the voltammograms were performed with PS trace software (PalmSens) by using the scientific mode. The amperograms were plotted using OriginPro 2020 software. The experimental setup for the flow injection analysis experiments is shown in Figure 6.

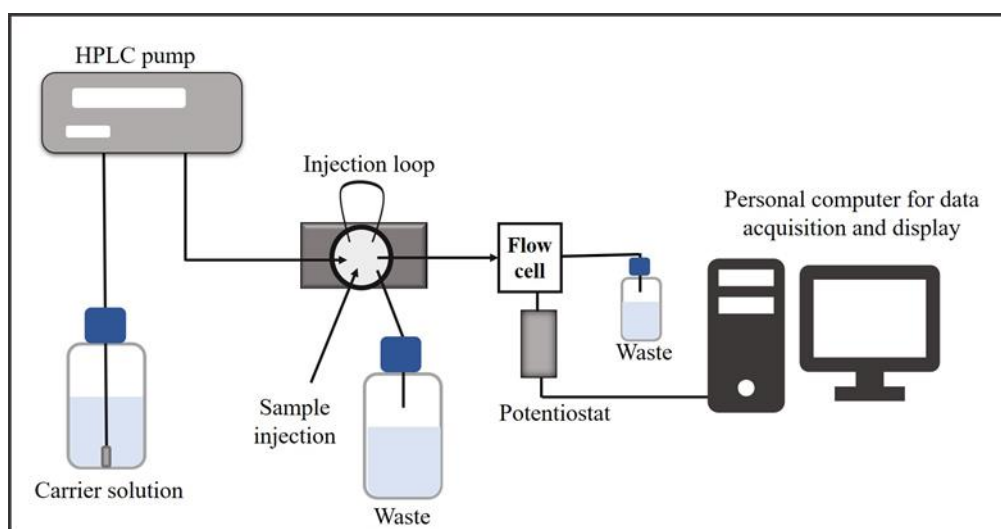Figure 6: The experimental setup for the flow injection analysis experiments.

To reduce the noise during the experiments and sparks while recording the amperometric measurements, some components of the flow injection analysis system were manually connected to a common ground bus that is grounded to one point. Figure 7 demonstrates the ground bus used in the flow injection analysis experiments.
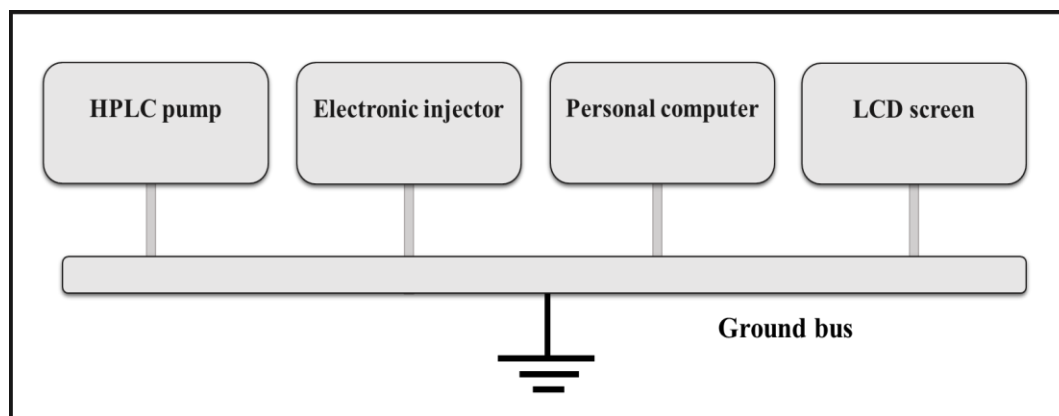
Figure 7: The ground bus used in flow injection analysis experiments.

Chapter 3: Results and Discussion

The fabrication technique developed in this project provides users an alternative fabrication technique to screen-printing technology. Although plating the commercial screen-printed electrode is possible, yet they cannot be harshly mechanically polished with sandpapers. On the other hand, the electrodes fabrication procedure described in this project allows the user to regenerate the electrodes by mechanical polishing prior to re-electroplating. This advantage has useful consequences: (i) in case the common electroplating problems occurred during the plating process such as dullness, blistering, and the formation of black marks, the situation can be fixed simply by doing some polishing and repeating the plating again, (ii) the ability to polish the electrodes, enables the user to work with just one single electrode yet changing the metallic coatings each time as per the requirements of the user's experiments.

3.1 Milling and Cutting Electrode's Board using the CNC Machine

Different strips with the different designs were obtained after milling and cutting as shown in Figure 8 to 10. The choice of the designs is up to the users. However, it should be noted that the small size end mill bits (1 mm diameter) for the CNC machine that are used to mill designs of small features can break. To avoid the small bits breaking they are used at high rotation speeds (e.g., 22,000 RPM).
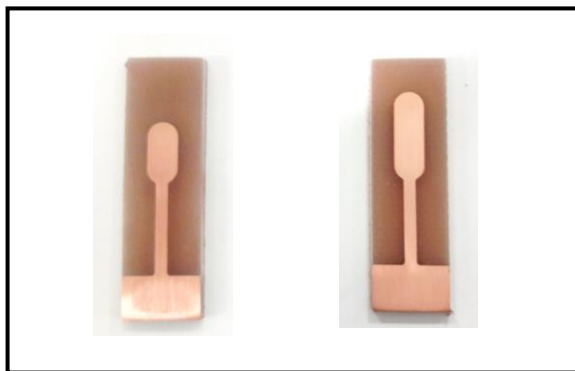
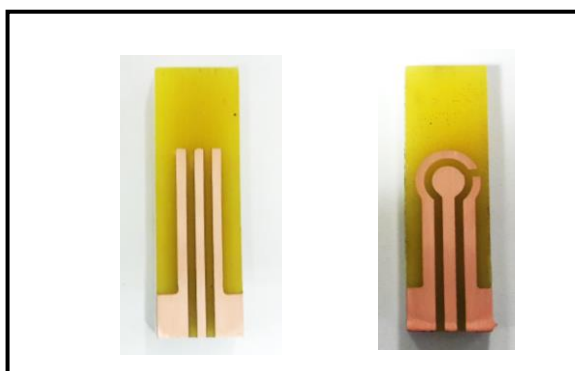Figure 8: The manufactured planar electrode A (left) and B (right) before electroplating.

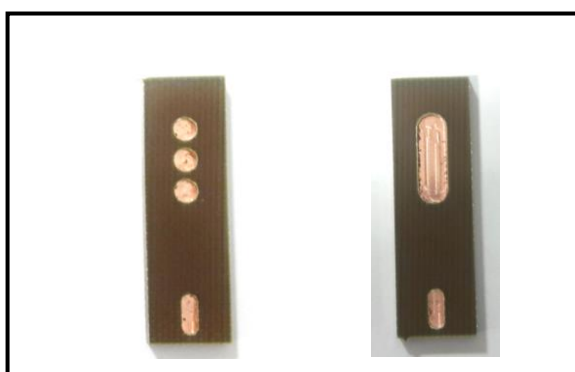Figure 9: The manufactured planar electrode C (left) and D (right) before electroplating.

Figure 10: The manufactured planar electrode E (left) and F (right) for modified carbon electrodes.

3.2 Electroplating of the Electrodes using Commercial Electroplating Baths

Different metallic coatings on the different planar electrodes were obtained after plating with the commercial electroplating baths. An example of an electrochemically plated gold electrode can be found in Figure 11. The electrodes A and B were used in the cyclic voltammetry experiments because they have one electrode which facilitates the plating process. While electrodes C and D have three electrodes on one strip which consumes more time to ensure perfect plating.
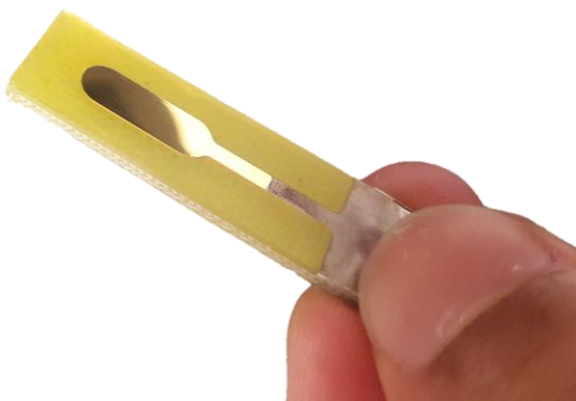
Figure 11: An example of a gold layer electrochemically plated on planar electrode B using commercial gold tank plating solution.

3.3 Characterizing the Planner Electrodes using Electroanalytical Methods

Cyclic voltammograms are described as the electrochemical spectra (Smith, Campbell, & Walsh, 1995). In this study, the cyclic voltammograms were done for solid metallic electrodes and their electroplated counterpart's electrodes to compare the electrochemistry of the electroplated layers with the real metals.

The cyclic voltammogram of the copper planar electrode was done to locate its characteristic redox peaks as shown in Figure 12. And to detect the presence of any

copper traces on the surface of the different metallic coatings produced. According to Giri and Sarkar (2016), the shoulder before peak A in Figure 12 is believed to be due to the formation of $Cu(OH)_2^-$, while peak A is believed to be due to the formation of Cu_2O. Peak B1 is also attributed to be due to the formation of insoluble $Cu(OH)_2$ and soluble $Cu(OH)_4^{2-}$ while peak B2 is primarily due to the formation of CuO. In the cathodic scan, peak C is claimed to mainly be due to the reduction of CuO to metallic copper. It was reported in the literature that at lower scan rates peak D gets broadened and segregated into multiple peaks. Peak D is probably due to the reduction of some soluble species entrapped inside the pores, the reduction of remaining oxides, and the reduction of the oxidation products during peak B1 (Giri & Sarkar, 2016).
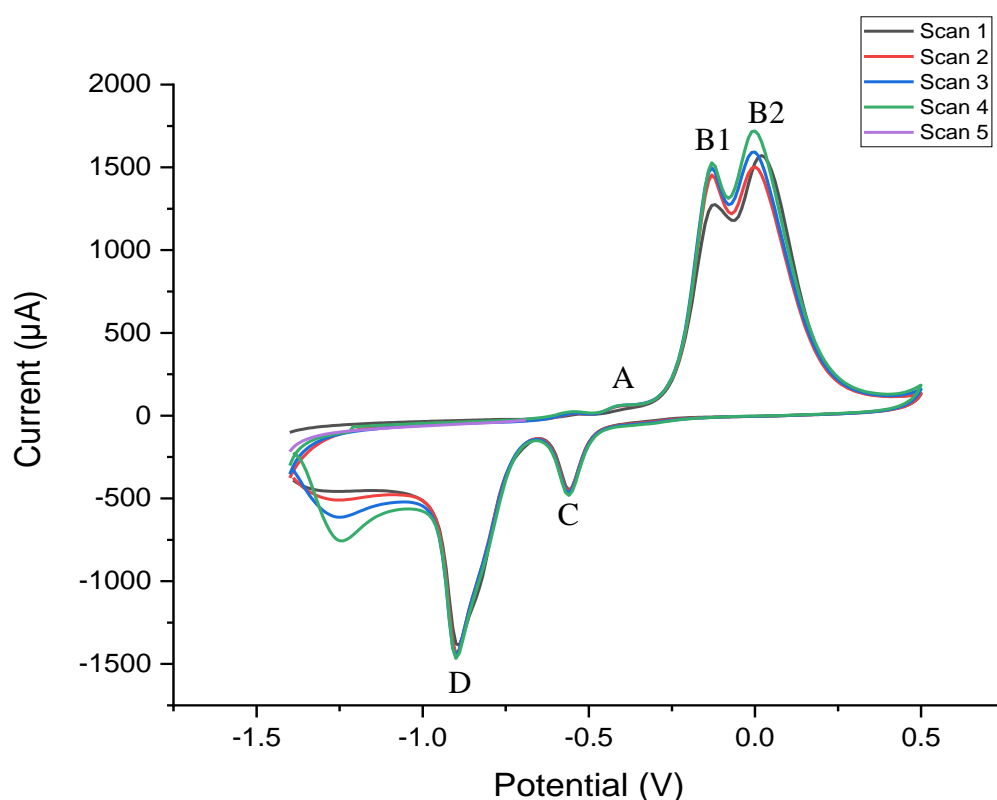

Figure 12: CV of Cu planar electrode (without any electroplating) in 0.5 M NaOH. Vs. Ag/AgCl. Scan rate = 0.05 V/s.

By comparing the cyclic voltammograms for gold in Figure 13 A with 13 B, silver in Figure 14 A with 14 B, and nickel in Figure 15 A with 15 B, the similarities between the cyclic voltammograms of the plated electrodes and their solid metallic electrodes counterparts revealed that electroplating of the different metals was done successfully. As a result, these plated electrodes are expected to have similar electrochemistry to their counterpart solid metallic electrodes yet at a cheaper cost.

Figures 13 A and B show the cyclic voltammograms for solid gold and gold-plated electrodes, respectively. The anodic peak A corresponds to the formation of gold oxide and the cathodic peak B corresponds to the reduction of gold oxides (Foguel et al., 2016). However, in Figure 13 B there is a peak C that appears in the anodic scan centered at around 0.2 V that is due to the double layer charge in which it decreases by continuous cycling. This behavior was also observed by (Foguel et al., 2016).

Figure 13: CVs of Au electrodes A) solid Au electrode and B) electrochemically Au-plated planar electrode. Both were measured in 0.5 M H_2SO_4 Vs. Ag/AgCl using a scan rate of 0.1 V/s. In B) the planar electrode was electrochemically plated with a layer of Ag using Ag tank solution, then with Au using Au tank solution for 6 times each time for 3 minutes, and polished with polishing cloth between each plating process. The final layer was polished with Au polish and then washed with detergent.

Figure 14 A and B show cyclic voltammogram related to silver metal. Peak A can be attributed to the formation of Ag_2O (Burstein & Newman, 1980, as cited in Abd El Rehim, Sayed S., Hassan, Ibrahim, & Amin, 1998; Amile et al. 1965; Muller & Smith, 1980, as cited in Abd El Rehim et al., 1998). The shoulder peak B could be due to the formation of AgO by different mechanisms (Tilak et al., 1972, as cited in Abd El Rehim et al., 1998; Stonehart, 1968, as cited in Abd El Rehim et al., 1998; Hoar & Dyer, 1972 as cited in Abd El Rehim et al., 1998; Dirkse & de Vries, 1959 as cited in Abd El Rehim et al., 1998; Fleischmann et al., 1968 as cited in Abd El Rehim et al., 1998; Brezina et al., 1968 as cited in Abd El Rehim et al., 1998). While in the cathodic scan, peak C could be due to the reduction of AgO to Ag_2O while peak D could be related to processes involved in the reduction of Ag(I) oxygen species to Ag (Abd El Rehim et al., 1998; Grozdić & Stojić, 1999; Wan et al., 2013).
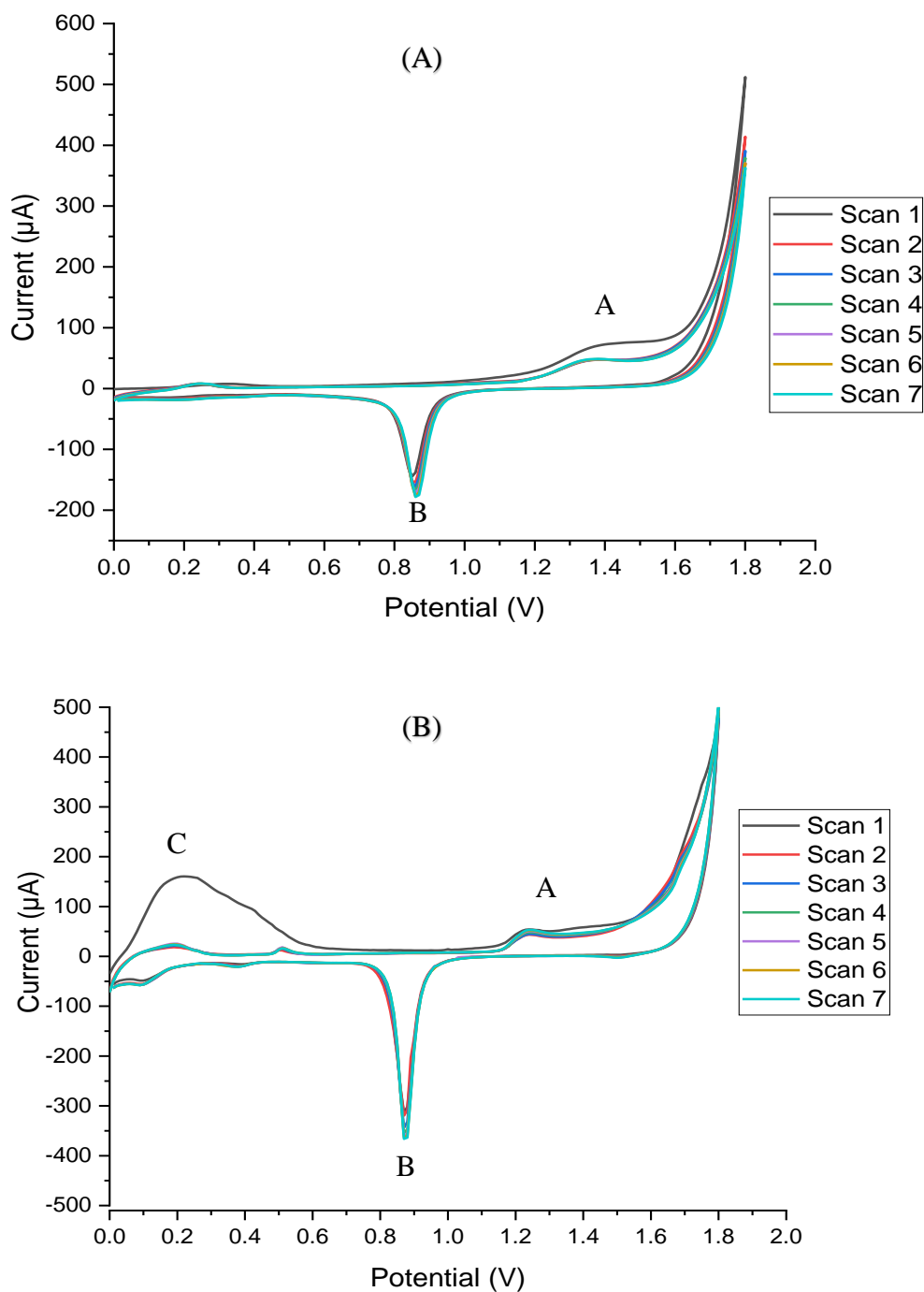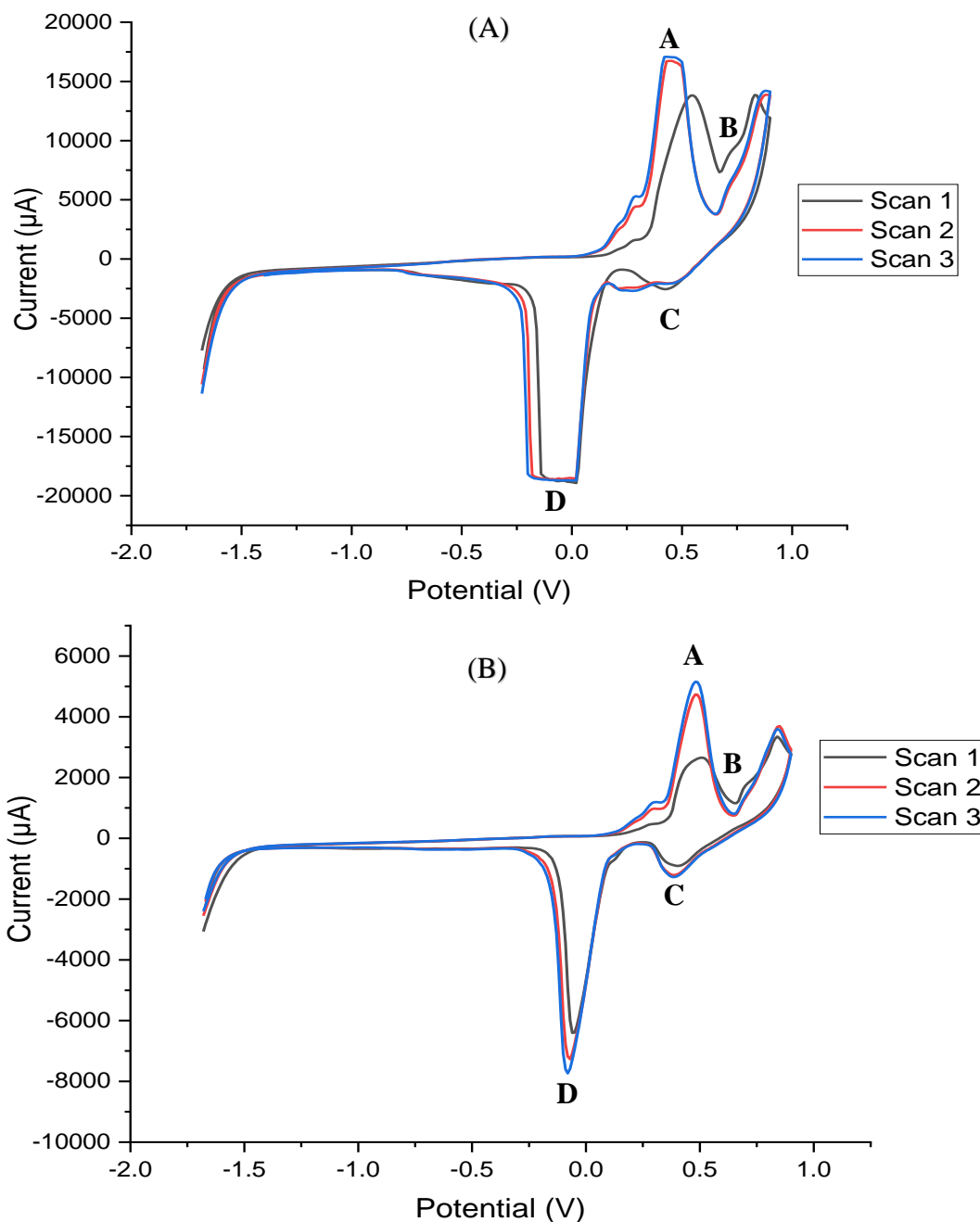
Figure 14: CVs of Ag electrodes A) Ag wire electrode and B) electrochemically Ag-plated planar electrode. Both were measured in 0.5 M NaOH Vs. Ag/AgCl using a scan rate of 0.1 V/s. In B) after polishing, the diamond paste was not applied, instead, the electrode was sonicated in ethanol for 15 minutes. Then, a layer of Au using Au strike solution was plated for 5 minutes followed by Ag using Ag tank solution for a total of 10 minutes. After the first 6 minutes, it was removed and polished with polishing cloth then the plating process was continued.

Figures 15 A and 15 B present the cyclic voltammograms for solid nickel and nickel-plated electrodes, respectively. The anodic peak at around 0.55 V is due to the oxidation of $Ni(OH)_2$ to NiOOH (Bode et al., 1966 as cited in Pissinis, Sereno, & Marioli, 2011). While the cathodic peak at around 0.4 V is due to the reduction of β-NiOOH (Marioli et al., 1996 as cited in Pissinis et al., 2012).
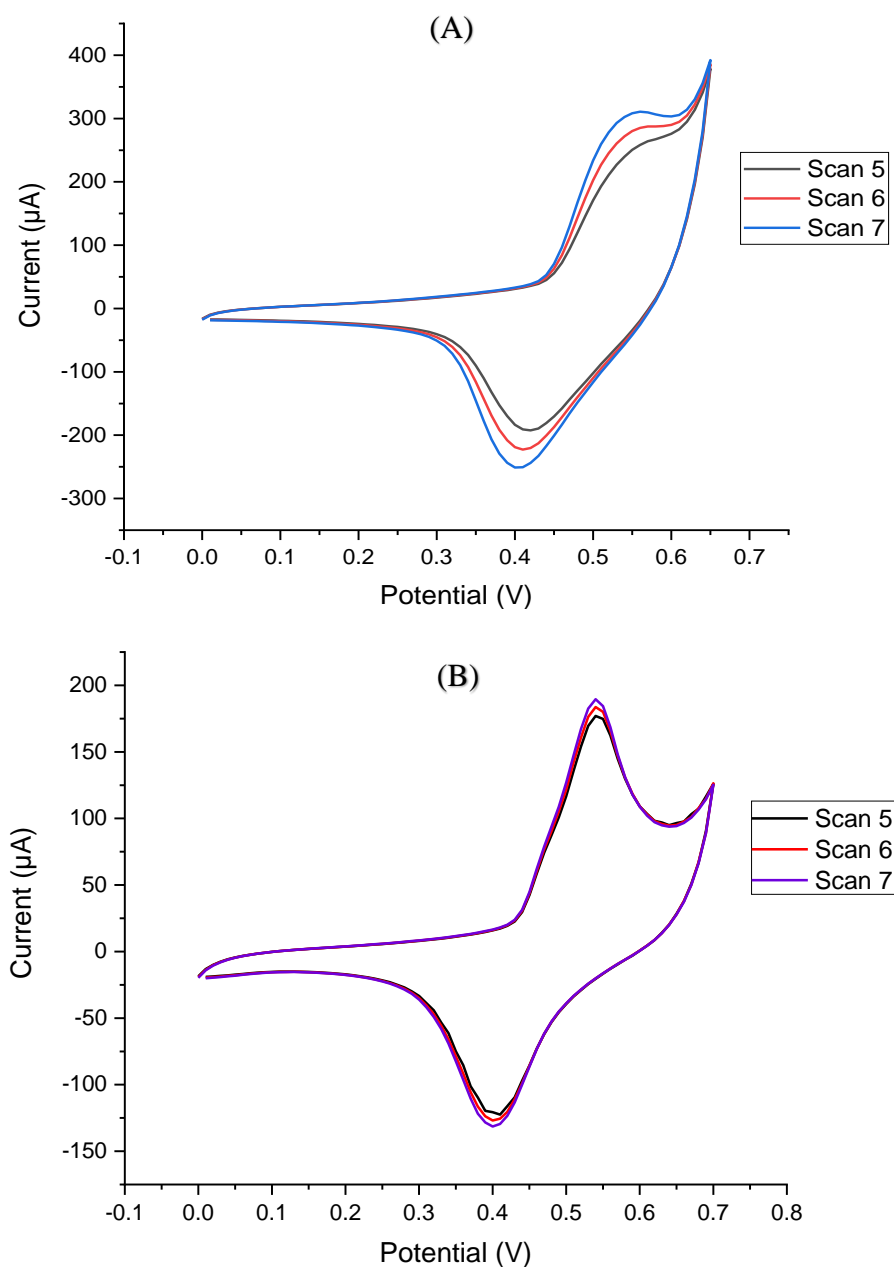
Figure 15: CVs of Ni electrodes. A) solid Ni electrode at scan rate of 0.05 V/s and B) electrochemically Ni-plated planar electrode at scan rate of 0.1 V/s. Both were measured in 0.1 M NaOH Vs. Ag/AgCl. In B) the planar electrode was electrochemically plated with a layer of Ag using Ag tank solution for 2 minutes then with Ni using Ni tank solution for 3 times each time for 2 minutes.

Figure 16 A and B show cyclic voltammograms related to platinum metal. In the anodic scan in Figure 16 A of the solid platinum electrode, region A is attributed to the adsorption of hydrogen, followed by region B which is the double layer region and lastly the oxide region C where the formation of monolayer oxide takes place (Ureta-Zanartu, Montenegro, & Zagal, 2001). While in the cathodic scan, region D is due to oxide reduction (Yang & Denuault, 1998 as cited in Ureta-Zanartu et al., 2001) (Villiard & Jerkiewicz, 1997 as cited in Ureta-Zanartu et al., 2001) and then followed by the hydrogen desorption region E (Ureta-Zanartu et al., 2001). The plated-platinum planar electrode shown in Figure 16 B is not similar to the cyclic voltammogram of the solid platinum electrode shown in Figure 16 A. To investigate this behavior, the potential window was minimized.
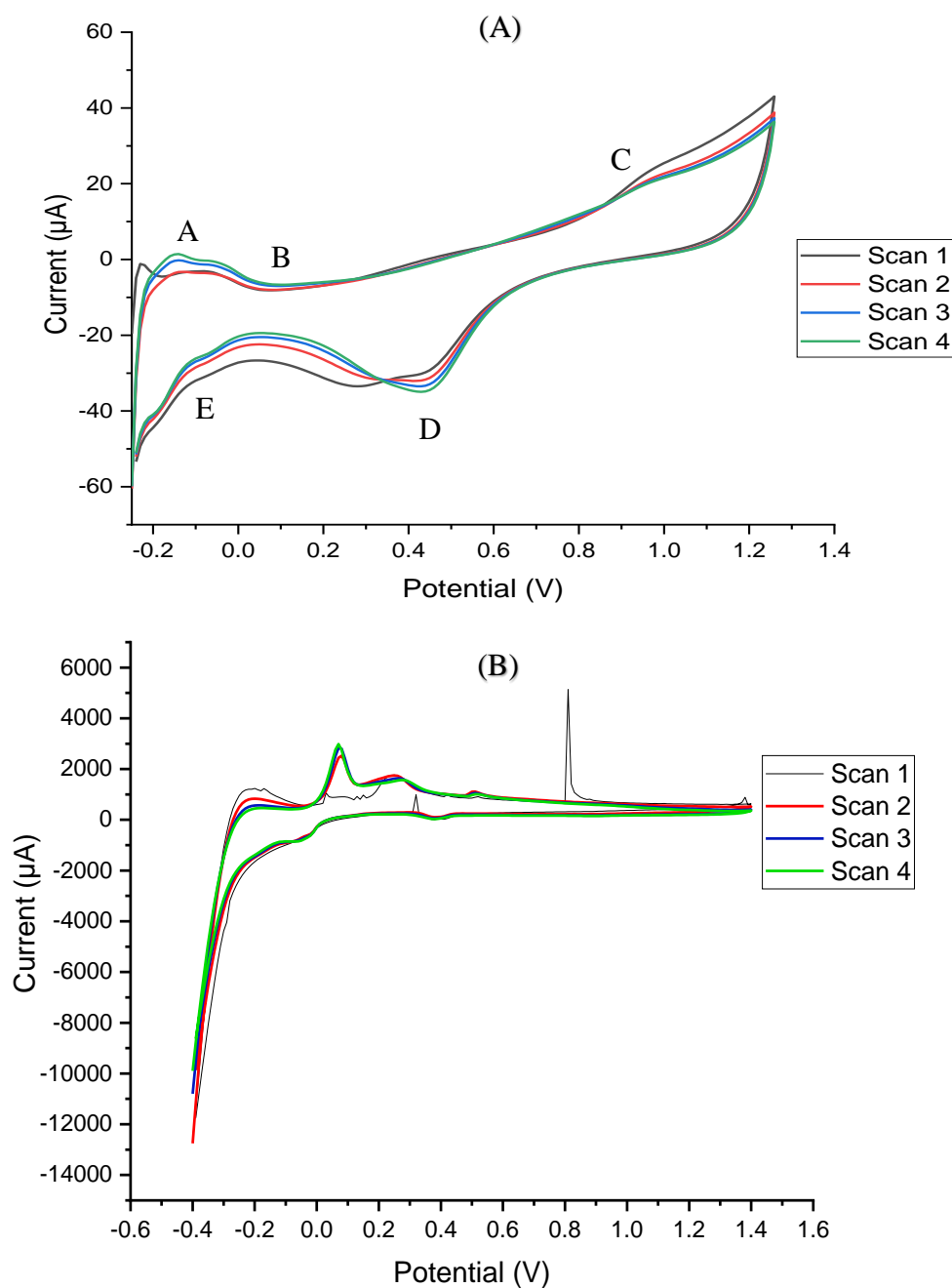
Figure 16: CVs of Pt electrodes A) solid Pt electrode and B) electrochemically Pt-plated planar electrode. Both were measured in 0.5 M H_2SO_4 Vs. Ag/AgCl using a scan rate of 0.1 V/s. In B) the electrode was polished with; the electric car polisher, then with 2000 grit sandpaper; washed with detergent; sonicated in ethanol for 15 minutes; electrochemically plated with a layer of Ag using Ag tank solution for 2 minutes, then with Au using Au tank solution for 6 minutes; polished with the polishing cloth; plated with a thin layer of Pt using the plating pen; then plated with Pt using Pt tank plating for 14 minutes and 21 seconds.

The potential window was minimized so to cover the range from 0.0 V to 1.2 V using the same planar electrode used in Figure 16 B. The result of this cyclic voltammetry is shown in Figure 17 A and the second scan is shown alone in Figure 17 B for clarity purpose. The effect of minimizing the potential window enhanced the result and the obtained cyclic voltammogram shown in Figure 17 (excluding the first scan) is similar to the reported cyclic voltammogram by (Hu & Liu, 1999) for their type-III platinum deposits on a titanium substrate.
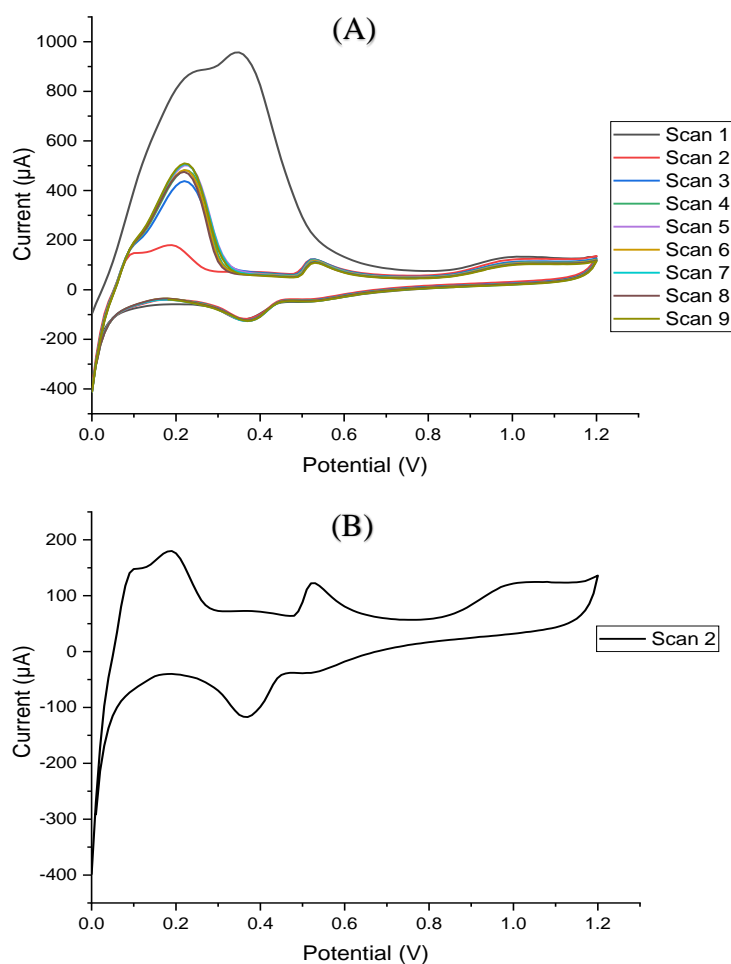
Figure 17: CV of electrochemically Pt-plated planar electrode using the same electrode in Figure 16 B. But scanned in a lower potential window. It was done in 0.5 M H_2SO_4 using a scan rate of 0.1 V/s. Vs. Ag/AgCl. A) Scans from 1 to 9. B) Scan 2 only presented for clarity purpose.

3.4. Examining the Edge's Effect on the Behavior of the Electrochemical Plating

The second step to understand the behavior of the platinum-plated electrodes was to investigate the edge effect on the behavior of the electrochemical plating. A recognizable enhancement was achieved in the cyclic voltammogram of the platinum-plated copper rod electrode after the insulation of its boundaries as shown in Figure 18 B when compared to its cyclic voltammogram before the insulation of its boundaries as shown in Figure 18 A.
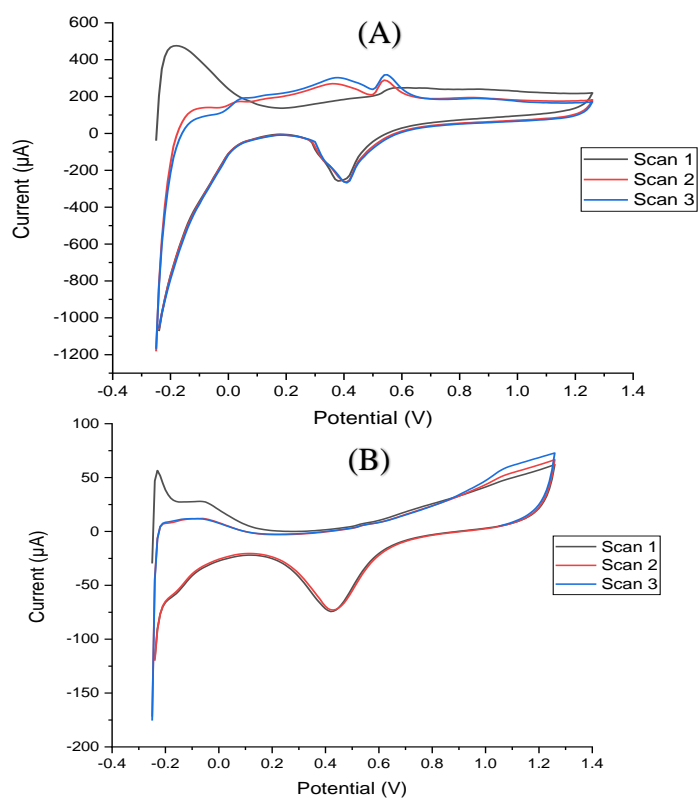
Figure 18: Edge effect experiments using the Cu rod electrode. A) CV of electrochemically Pt-plated copper rod electrode plated with the plating pen with Ni, Au, Ag, Au, then Pt. B) After cycling the electrode in A, it was plated with additional layer of Au followed by Pt using the plating pen; the edges were insulated using a nail polish; then it was cycled again. Both CVs were done in 0.5 M H_2SO_4 Vs. Ag/AgCl using a scan rate of 0.1 V/s.

Similar behavior was observed with the planar platinum-plated electrode as shown in Figures 19 A and B. However, the edge effect was more pronounced in the case of the planar platinum-plated electrode as the cyclic voltammogram shown in Figure 19 A differs immensely from the cyclic voltammogram of real solid platinum electrode shown in Figure 16 A.
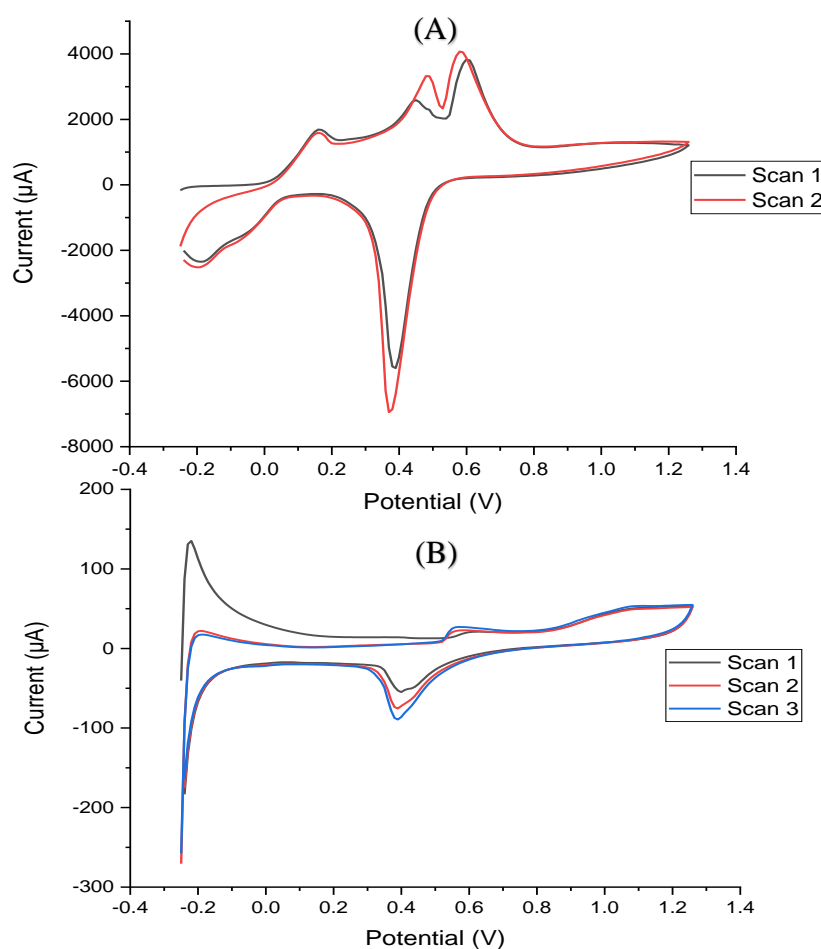
Figure 19: Edge effect experiments using the Cu planar electrode. A) CV of the electrochemically Pt-plated copper planar electrode (oval shape) plated with the plating pen with Ni, Au, Ag, Au, then Pt. Before the plating was done, the electrode was polished with sandpaper, then with the Dremel® polisher with some diamond paste, and then sonicated in deionized water. B) After cycling the electrode in A, it was plated with an additional layer of Au followed by Pt using the plating pen; and the edges were insulated using a nail polish. Lastly, it was cycled again. Both CVs were done in 0.5 M H_2SO_4 Vs. Ag/AgCl using a scan rate of 0.1 V/s.

This could be attributed to the fact that the edge between the copper and the epoxy in the case of the planar electrode has some cracks while this edge is not presented in the copper rod electrode. Platinum has the tendency to absorb molecular hydrogen thus causing hydrogen liberation and hydrogen embrittlement which is a major concern for low pH plating baths (Rao & Trivedi, 2005) and the used Pt bath has a low pH. Consequently, the edge effect that was observed in the case of platinum electroplating on the planar electrode could be due to the combined effect of having some cracks between the copper and the epoxy layer with the effect of hydrogen gas formation. This edge effect could affect the performance and the stability of the electrodes as will be discussed in the stability test results section (3.5.3).

3.5 Application of the Fabricated Electrodes in Flow Injection Analysis

3.5.1 The H₂O₂ Experiments using the D Electrode

The amperometric responses of the D electrode towards H_2O_2 detection at flow rates of 0.5, 1.0, and 1.5 ml/min are shown in Figures 20 to 22. It should be noted that the data shown in Figures 20 to 22 are baseline subtracted. At flow rate 1.0 ml/min, the limit of detection was estimated to be 38.4 µM and the limit of quantitation was estimated to be 116.4 µM using the linear regression method as shown in the equations below (Shrivastava & Gupta, 2011):

LOD = 3 x (Standard deviation of the response/sensitivity)   (1)

LOQ = 10 x (Standard deviation of the response/sensitivity)   (2)

The standard deviation of the response was estimated by the standard deviation of the y-intercept and the sensitivity is the slope of the calibration curve (Shrivastava & Gupta, 2011).

Figure 20: FIA amperometric response of the D electrode for H_2O_2 standard solutions at a flow rate of 0.5 ml/min. Carrier solution: 0.1 M PBS pH (7.0). Sample loop volume: 100 μl. E: +0.7 V. The curve is baseline subtracted. The baseline value is 7.65 μA.

Figure 21: FIA amperometric response of the D electrode for H_2O_2 standard solutions at a flow rate of 1.0 ml/min. Carrier solution: 0.1 M PBS pH (7.0). Sample loop volume: 100 μl. E: +0.7 V. The curve is baseline subtracted. The baseline value is 6.25 μA.
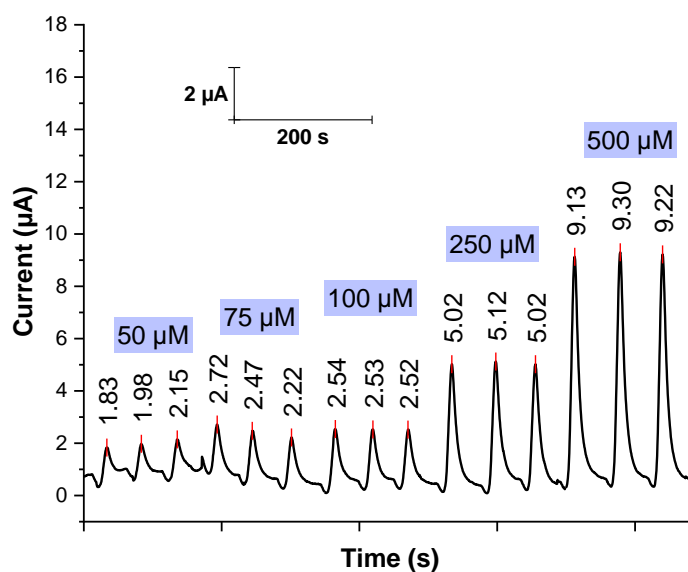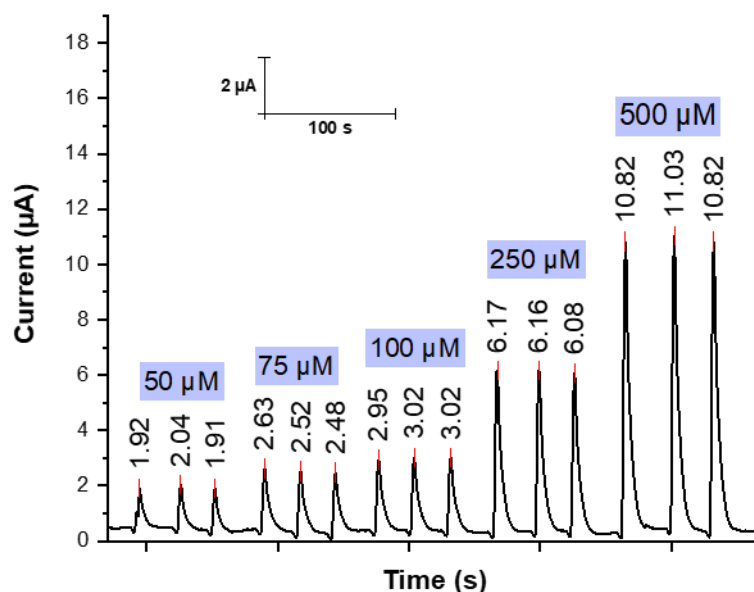
Figure 22: FIA amperometric response of the D electrode for H_2O_2 standard solutions at a flow rate of 1.5 ml/min. Carrier solution: 0.1 M PBS pH (7.0). Sample loop volume: 100 μl. E: +0.7 V. The curve is baseline subtracted. The baseline value is 6.25 μA.
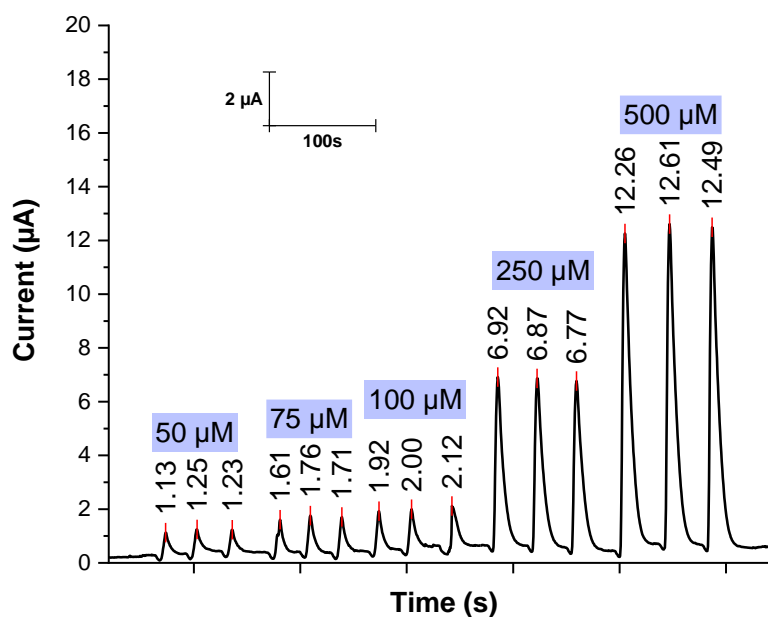
The calibration curves at the three different flow rates were plotted in one curve for comparison as shown in Figure 23. The plotted points in the calibration curves shown in Figure 23 are the average of three peak maxima for each concentration obtained from the subtracted data in Figures 20 to 22. The highest slope was obtained at 1.0 ml/min. The lower slopes observed as lower and higher flow rates could be attributed to the excessive sample dispersion and the incomplete response (because of the shorter residence time), respectively.

Figure 23: Calibration curves of H_2O_2 using the D electrode FIA amperometric responses at different flow rates. Carrier solution: 0.1 M PBS pH (7.0). Sample loop vo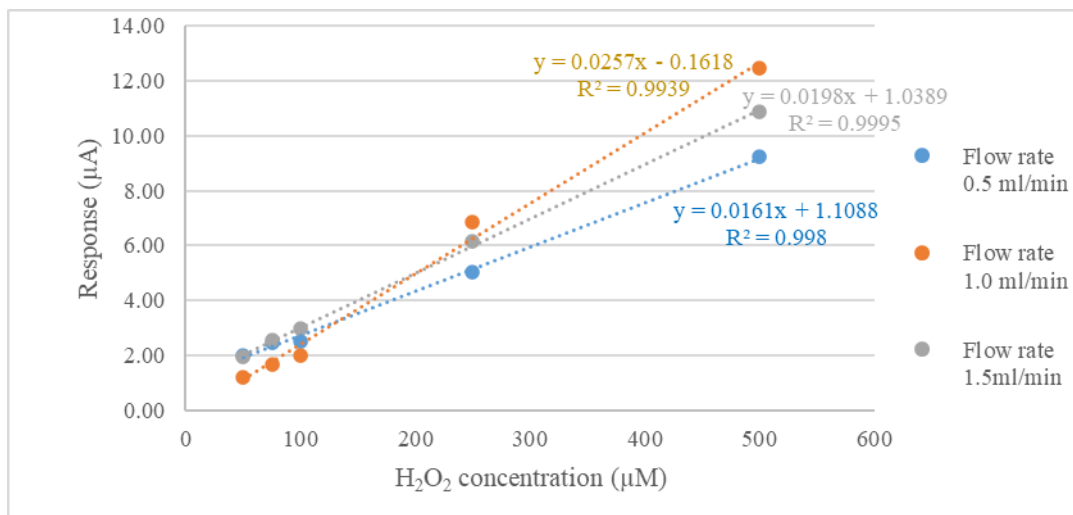lume: 100 μl. E: +0.7 V. The response in the y-axis is the average of three peak maxima for each concentration. The peak maxima were obtained from the baseline subtracted curves shown in Figures 20, 21, and 22.

3.5.2 The H₂O₂ Experiments using the C Electrode

The amperometric response of the C electrode toward H_2O_2 detection at flow rate 0.5, 1.0, and 1.5 ml/min are shown in Figures 24 to 26. It should be noted that the data shown in Figures 24 to 26 are baseline subtracted. At a flow rate of 1.0 ml/min, the limit of detection was estimated to be 48.5 µM while the limit of quantitation was estimated to be 161.8 µM using the linear regression method described previously in equation (1) and (2) in which the standard deviation of the response was estimated by the standard deviation of *y*-intercept (Shrivastava & Gupta, 2011).

Figure 24: FIA amperometric response of the C electrode for H_2O_2 standard solutions at a flow rate of 0.5 ml/min. Carrier solution: 0.1 M PBS pH (7.0). Sample loop volume: 100 µl. E: +0.7 V. The curve is baseline subtracted. The baseline value is 3.6 µA.

Figure 25: FIA amperometric response of the C electrode for H_2O_2 standard solutions at a flow rate of 1.0 ml/min. Carrier solution: 0.1 M PBS pH (7.0). Sample loop volume: 100 μl. E: +0.7 V. The curve is baseline subtracted. The baseline value is 3μA.
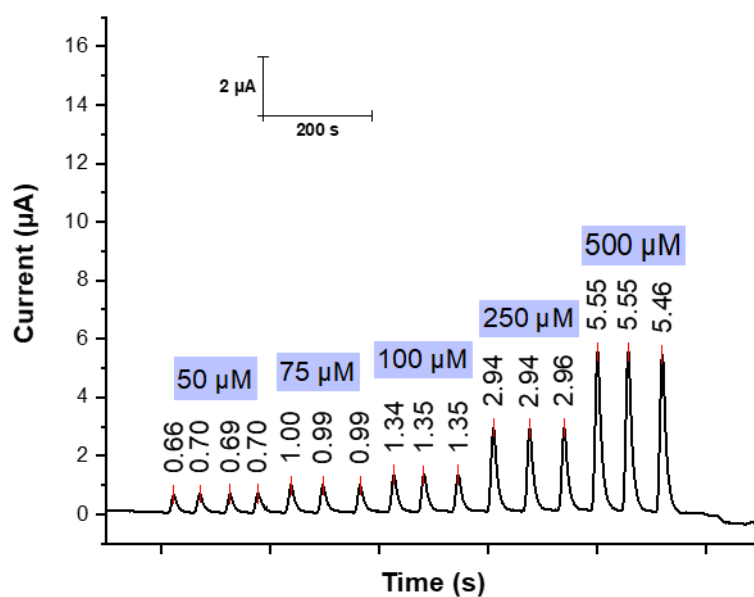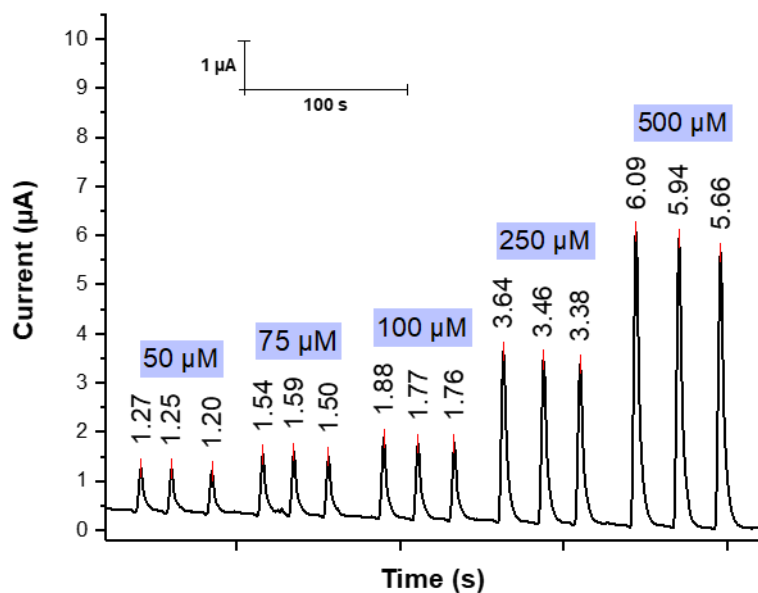

Figure 26: FIA amperometric response of the C electrode for H_2O_2 standard solutions at a flow rate of 1.5 ml/min. Carrier solution: 0.1 M PBS pH (7.0). Sample loop volume: 100 μl. E: +0.7 V. The curve is baseline subtracted. The baseline value is 3μA.
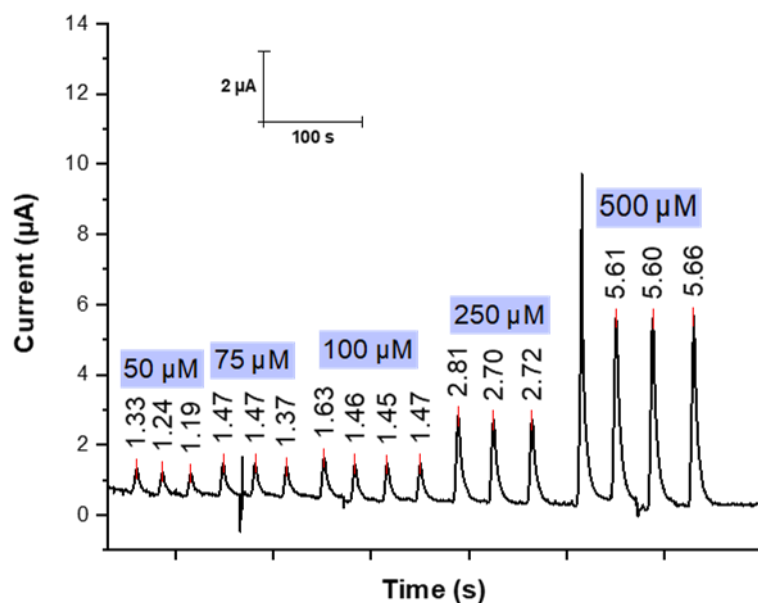
The calibration curves at flow rates 0.5, 1.0, 1.5 ml/ min were plotted in one curve for comparison as shown in Figure 27. The plotted points in the calibration curves shown in Figure 27 are the average of three peak maxima for each concentration obtained from the subtracted data in Figure 24 to 26.
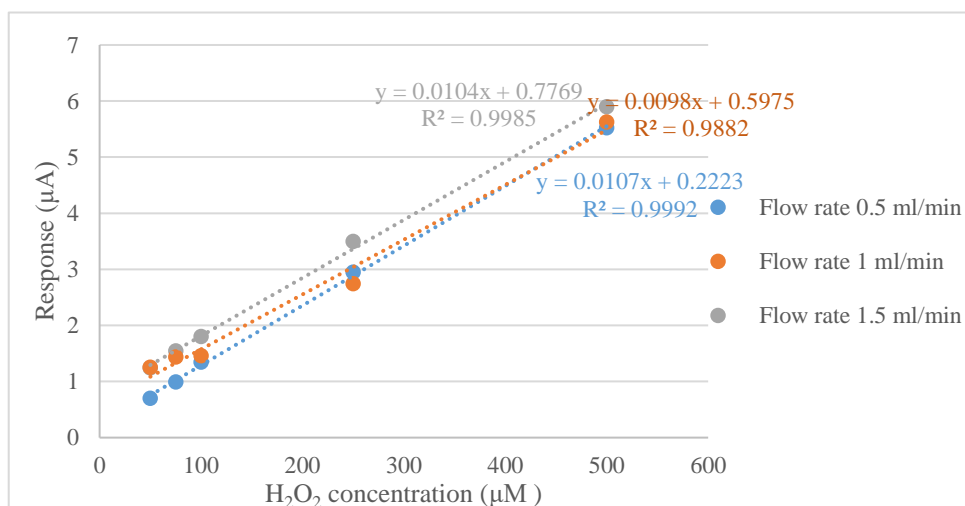
Figure 27: Calibration curves of H_2O_2 using the C electrode FIA amperometric responses at different flow rates. Carrier solution: 0.1 M PBS pH (7.0). Sample loop volume: 100 μl. E: +0.7 V. The response in the y-axis is the average of three peak maxima for each concentration obtained from the baseline subtracted curves shown in Figures 24, 25, and 26.

The D electrode has lower limits of detection and quantitation than the C electrode. This could be attributed to the differences in the geometrical area between the two electrodes. The limitations of the plating process will be discussed in the stability test section (3.5.3). The described amperometric method for the detection of hydrogen peroxide using C and D electrodes in this work show lower LOD compared to some other methods that are reported in the literature as shown in Table 1.

Table 1: A comparison of LODs for different H_2O_2 detection methods using different electrodes.

Electrode	LOD (μM)	Electrochemical technique	Reference
Immobilized peroxidase (from the leaves of Guinea grass) on screen-printed graphene electrode	150	Reduction of H_2O_2 Amperometry Not FIA	(Centeno, Solano, & Castillo, 2017)
Carbon paste electrode modified with Co_2SnO_4	65.38	Reduction of H_2O_2 Amperometry Not FIA	(Mosquera et al., 2017)
Pt nanoflower deposited on gold film	60	Oxidation of H_2O_2 Amperometry Not FIA	(Wan, Wang, Yin, & Ma, 2012)
C electrode in this work	48.5	Oxidation of H_2O_2 Amperometry FIA	This work
D electrode in this work	38.4	Oxidation of H_2O_2 Amperometry FIA	This work

3.5.3 The Stability Test

The result of the response stability experiment for D electrode is shown in Figure 28. The curve in Figure 28 is not baseline subtracted.

Figure 28: Response stability of the D electrode. Standard solution concentration: 100 μM H_2O_2. Carrier solution: 0.1 M PBS pH (7.0). Flow rate: 1.0 ml/min. Sample loop volume: 100 μl. E: +0.7 V. The curve is not baseline subtracted.

And the result of the response stability experiment of the C electrode is shown

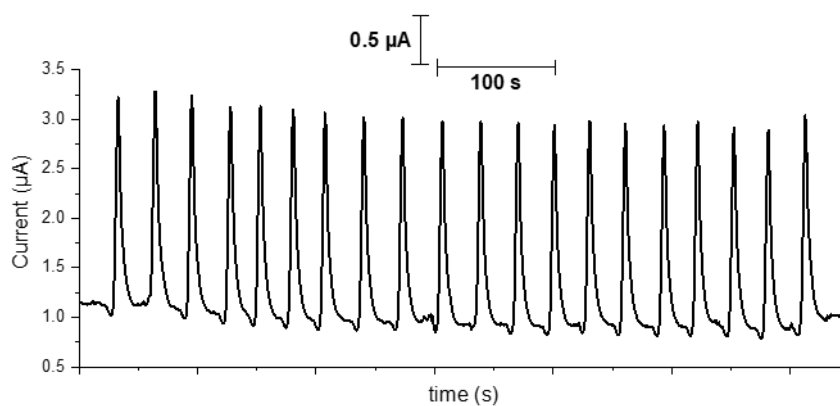in Figure 29. The curve in Figure 29 is not baseline subtracted.
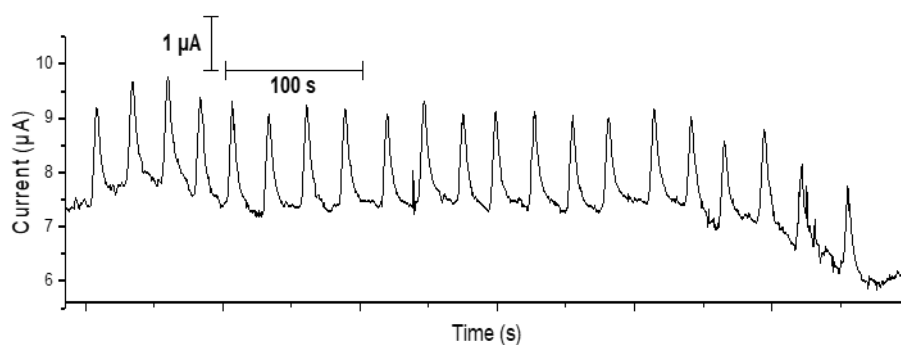

Figure 29: Response stability of the C electrode. Standard solution concentration: 100 μM H_2O_2. Carrier solution: 0.1 M PBS pH (7.0). Flow rate: 1.0 ml/min. Sample loop volume: 100 μl. E: +0.7 V. The curve is not baseline subtracted.

Nothdurft and coauthors (2019) nicely reviewed the manufacturing and interfacial failure mechanisms for copper/epoxy joints in printed circuit boards (Nothdurft, Riess, & Kern, 2019). According to their discussion, the interphase between the epoxy and the copper can be judged as a source of weakness. It can be a place where water/water vapor get trapped (Tencer, 1994 as cited in, Nothdurft et al., 2019). The epoxy polymer may also get degraded by the formation of the cuprous/cupric ion which was found to be effective redox couple that accelerates the decomposition of polymers (Yoshida & Ishida, 1984 as cited in Nothdurft et al., 2019; Patrick, 1970 as cited in Nothdurft et al., 2019). All these factors could weaken the adhesion between the applied epoxy and the copper surface. Also, tiny contaminants that were left behind from the debris produced during the cutting process may still present at the edges and could weaken the adhesion between the copper and the epoxy. All this can reflect on the response stability of the electrodes since the edges at the in interphase will not be perfectly plated. Also, it could be explained that these sites can promote the peeling of the plated layer during the FIA experiments (which was observed). The condition of the FIA experiments involves a flow of a stream and an applied potential that also induce the peeling of the plated layers. When such peeling occurs on the electrode, its response is no more constant. Subsequently, the obtained baseline will not be stable.

C electrode has a less stable baseline in Figure 29 compared to the D electrode in Figure 28. The reason behind the differences in the stability is still unknown but this could be attributed to the fact that the area of the interphase in the C electrode is more than that in the D electrode.

3.5.4 Real Sample Injection

The amperogram of H_2O_2 detection using the D electrode is shown in Figure 30. It should be noted that the data shown in Figure 30 are baseline subtracted.
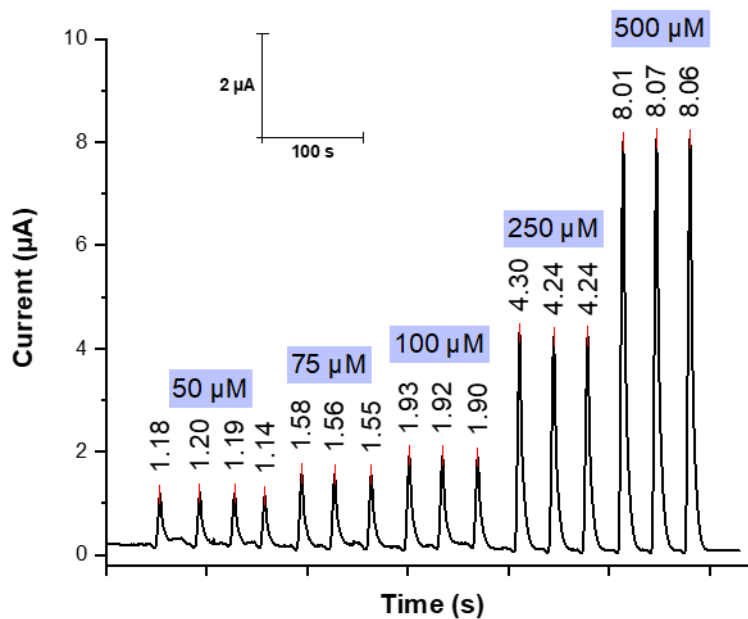
Figure 30: FIA amperometric response using the D electrode for H_2O_2 standard solutions at a flow rate of 1.0 ml/min made to construct a calibration curve to inject the hair developer sample. Carrier solution: 0.1 M PBS pH (7.0). Sample loop volume: 100 μl. E: +0.7 V. The curve is baseline subtracted. The baseline value is 0.45 μA.

The amperogram shown in Figure 30 was constructed again to plot a calibration curve as shown in Figure 31 for the as mentioned reason in the experimental section. The plotted points in Figure 31, are the average of the most three closest peak maxima for each concentration obtained from Figure 30.
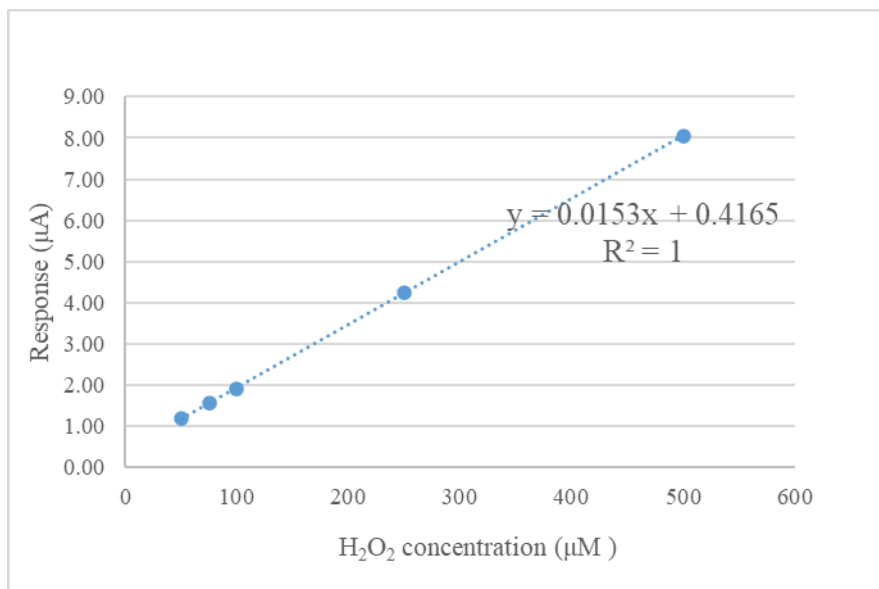
Figure 31: Calibration curve of H_2O_2 using the D electrode FIA amperometric responses at a flow rate of 1.0 ml/min. Carrier solution: 0.1 M PBS pH (7.0). Sample loop volume: 100 µl. E: +0.7 V. The response in the y-axis is the average of three peak maxima for each concentration obtained from the baseline subtracted curves shown in Figure 30.

The injection of the diluted hair developer sample using electrode D and electrode C are shown in Figure 32 and Figure 33, respectively. The average of the peak maxima for the triplicate injections of the diluted sample was used to estimate H_2O_2 concentration in the sample. For D electrode the estimated concentration of H_2O_2 after compensation for the dilution factor was found to be 1.08 M. While for C electrode the estimated H_2O_2 concentration in the sample was found to be 1.2 M.
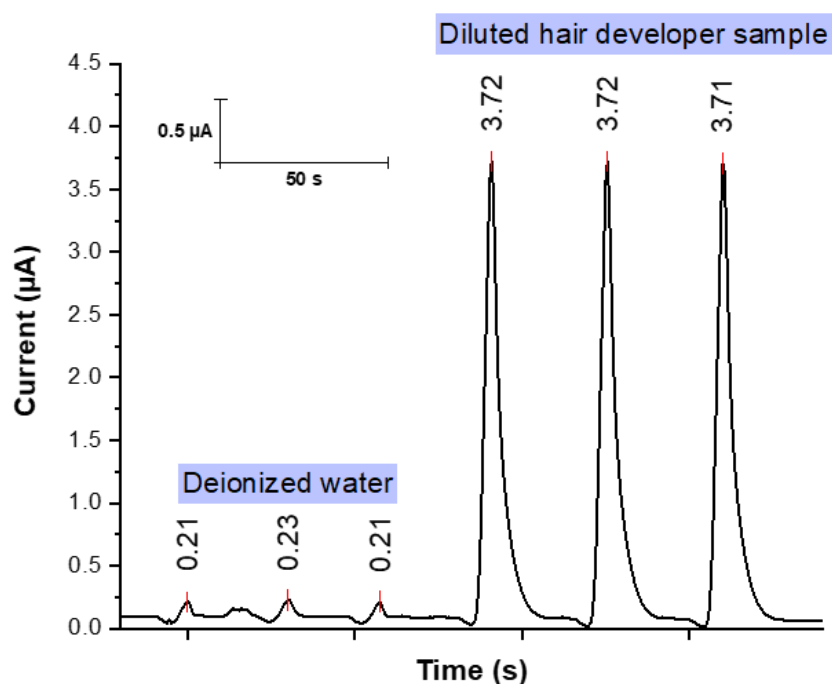
Figure 32: Diluted hair developer sample response recorded for H_2O_2 determination using the D electrode. The sample was diluted by a factor of 5000 in deionized water. Carrier solution: 0.1 M PBS pH (7.0). Flow rate: 1.0 ml/min. Sample loop volume: 100 μl. E: +0.7 V. The curve is baseline subtracted. The baseline value is 0.42 μA.
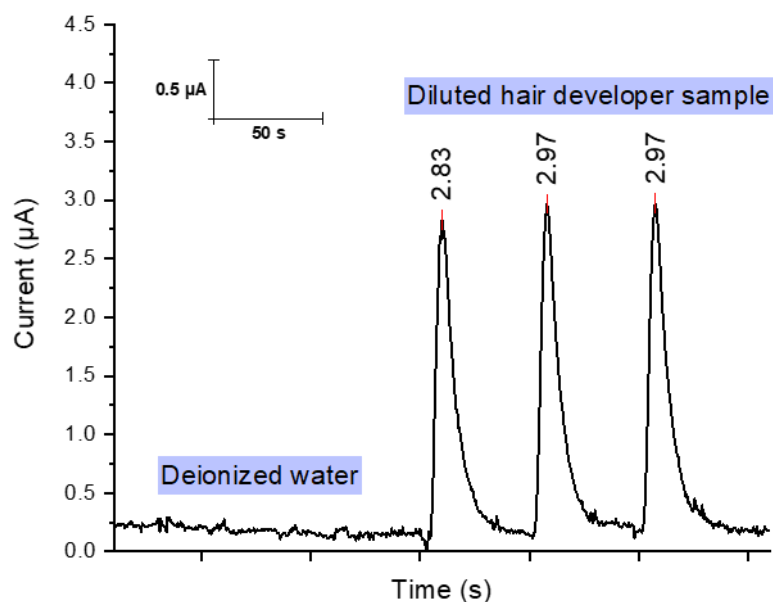
Figure 33: Diluted hair developer sample response recorded for H_2O_2 determination using the C electrode. The sample was diluted by a factor of 5000 in deionized water. Carrier solution: 0.1 M PBS pH (7.0). Flow rate: 1.0 ml/min. Sample loop volume: 100 μl. E: +0.7 V. The curve is baseline subtracted. The baseline value is 2.62 μA.

3.5.5 Preliminary Experiments on the Amperometric Detection of Glycerol

Excessive amounts of glycerol in biodiesel is not preferred because it can cause several problems. The glycerol will settle out in the storage tank making a highly viscous mixture. This highly viscous mixture can clog the fuel filters. Also, in the engine, it can cause combustion problems (Ferrari, Pighinelli, & Park, 2011). So, a sensor that is capable of detecting glycerol can be used in the quality control check of biodiesels (Maruta & Paixão, 2012). The amperometric response of the D electrode toward glycerol oxidation at a flow rate of 1.0 ml/min is shown in Figure 34. Copper without any electroplating was used as the working electrode while the final layer plated on the counter and reference electrode were platinum and silver, respectively. It should be noted that the data shown in Figure 34 is baseline subtracted.

Figure 34: FIA amperometric response of the D electrode for glycerol standard solutions at a flow rate of 1.0 ml/min. Carrier solution: 2 M NaOH. Sample loop volume: 100 μl. E: +0.65 V. The curve is baseline subtracted. The baseline value is 3.6 μA.

The amperometric response of the C electrode toward glycerol oxidation at a flow rate of 1.0 ml/min is shown in Figure 35. Copper without any electroplating was used as the working electrode while the final layer plated on the counter and reference electrode were platinum and silver, respectively. It should be noted that the data shown in Figure 35 is baseline subtracted. The differences in the responses (sensitivities) could be due to the instability of glycerol standard solutions of such low concentrations.
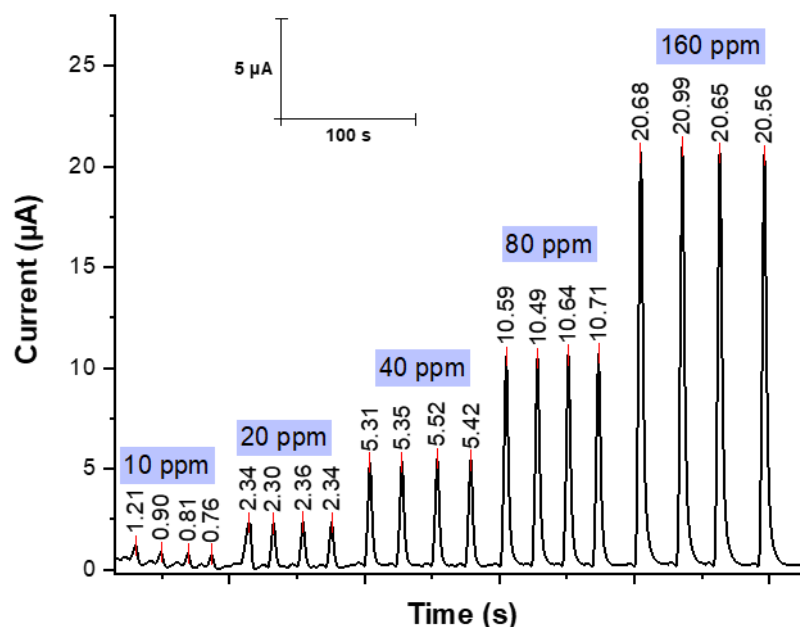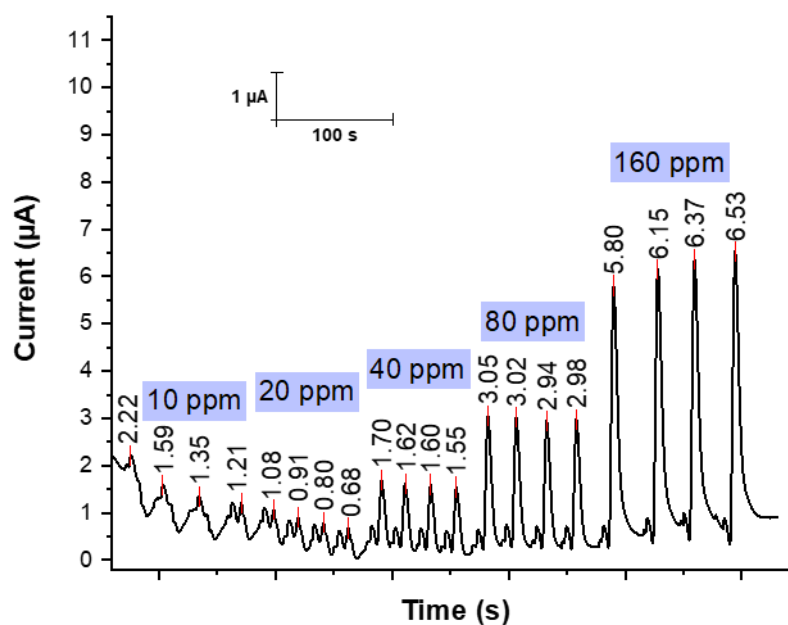

Figure 35: FIA amperometric response of the C electrode for glycerol standard solutions at a flow rate of 1.0 ml/min. Carrier solution: 2 M NaOH. Sample loop volume: 100 μl. E: +0.65 V. The curve is baseline subtracted. The baseline value is 4 μA.

Chapter 4: Conclusion

In this thesis, planar electrodes with different designs were manufactured using a CNC machine. The manufactured planar electrodes were electroplated with different metallic coatings to produce a variety of electrodes. The produced planar electrodes gave better reusability than the available screen-printed electrodes. Thanks to their ability to withstand harsh sandpaper polishing which allows the user to i) polish the electrodes and re-plate them again -in case the layer plated was damaged- thus increasing its lifetime ii) change the metallic coatings of the electrodes - i.e. gold, silver, nickel, platinum- as per the requirements of the user's experiments by just using one single strip. The produced planar electrodes in this work were able to successfully detect different analytes i.e. hydrogen peroxide and glycerol in flow injection analysis mode. Despite the advantages mentioned, there are some observed limitations: i) peeling of the electroplated layers during the flow injection analysis experiments, ii) the high precision needed when plating the strips that have three electrodes on them i.e. reference electrode, working electrode, and counter electrode to prevent the contact of the plating solution to adjacent electrode thus contaminating adjacent electrodes or plating them undesirably, iii) and the precision needed to plate the electrodes increases the time of electrode preparation.

Future work will include continuing the work with the manufactured cavity electrodes (E and F in the result and discussion section), by filling them with carbon paste and conducting carbon epoxy then experimenting their electrochemical behavior. And, studying the interphase between the copper and the epoxy resin to enhance the plating of the different metal on the copper in that region.

References

Abd El Rehim, S. S., Hassan, H. H., Ibrahim, M. A. M., & Amin, M. A. (1998). Electrochemical Behaviour of a Silver Electrode in NaOH Solutions. *Monatshefte Für Chemie / Chemical Monthly*, *129*(11), 1103–1117. https://doi.org/10.1007/PL00010123

Amlie, R. F., Honer, H. N., & Ruetschi, P. (1965). The Voltage Increase of the Cuprous Chloride Electrode by the Addition of Sulfur. *Journal of The Electrochemical Society*, *112*(11), 1073–1078. https://doi.org/10.1149/1.2423364

Antuña-Jiménez, D., González-García, B. M., Hernández-Santos, D., & Fanjul-Bolado, P. (2020). Screen-Printed Electrodes Modified with Metal Nanoparticles for Small Molecule Sensing. *Biosensors*, *10*(2), 9. https://doi.org/10.3390/bios10020009

Bard, A. J., & Faulkner, L. R. (2000). *Electrochemical methods: fundamentals and applications* (second). John Wiley & Sons, Inc.

Bergamini, M. F., Santos, A. L., Stradiotto, N. R., & Zanoni, M. V. B. (2007). Flow injection amperometric determination of procaine in pharmaceutical formulation using a screen-printed carbon electrode. *Journal of Pharmaceutical and Biomedical Analysis*, *43*(1), 315–319. https://doi.org/10.1016/j.jpba.2006.06.001

Bode, H., Dehmelt, K., & Witte, J. (1966). Zur kenntnis der nickelhydroxidelektrode—I.Über das nickel (II)-hydroxidhydrat. *Electrochimica Acta*, *11*(8), 1079–1087. https://doi.org/https://doi.org/10.1016/0013-4686(66)80045-2

Bond, A. M. (1994). Past, present and future contributions of microelectrodes to analytical studies employing voltammetric detection. A review. *Analyst*, *119*(11), 1R-21R. https://doi.org/10.1039/AN994190001R

Březina, M., Koryta, J., & Musilová, M. (1968). Electrode processes of oxygen and of hydrogen peroxide on a silver electrode in alkali hydroxide solution. *Collection of Czechoslovak Chemical Communications*, *33*(11), 3397–3409. https://doi.org/https://doi.org/10.1135/cccc19683397

Burstein, G. T., & Newman, R. C. (1980). Anodic behaviour of scratched silver electrodes in alkaline solution. *Electrochimica Acta*, *25*(8), 1009–1013. https://doi.org/https://doi.org/10.1016/0013-4686(80)87006-X

Centeno, D. A., Solano, X. H., & Castillo, J. J. (2017). A new peroxidase from leaves of guinea grass (Panicum maximum): A potential biocatalyst to build amperometric biosensors. *Bioelectrochemistry*, *116*, 33–38. https://doi.org/https://doi.org/10.1016/j.bioelechem.2017.03.005

Chyan, Y., & Chyan, O. (2008). Metal Electrodeposition on an Integrated, Screen-Printed Electrode Assembly. *Journal of Chemical Education*, *85*(4), 565-567. https://doi.org/10.1021/ed085p565

Cumba, L. R., Foster, C. W., Brownson, D. A. C., Smith, J. P., Iniesta, J., Thakur, B., … Banks, C. E. (2016). Can the mechanical activation (polishing) of screen-printed electrodes enhance their electroanalytical response? *Analyst*, *141*(9), 2791–2799. https://doi.org/10.1039/C6AN00167J

de Mattos, I. L., Gorton, L., & Ruzgas, T. (2003). Sensor and biosensor based on Prussian Blue modified gold and platinum screen printed electrodes. *Biosensors and Bioelectronics*, *18*(2-3), 193–200. https://doi.org/https://doi.org/10.1016/S0956-5663(02)00185-9

World Health organization. (2020). Diabetes. Retrieved May 23, 2020 from https://www.who.int/news-room/fact-sheets/detail/diabetes

Djordjevic, A. R., Biljié, R. M., Likar-Smiljanic, V. D., & Sarkar, T. K. (2001). Wideband frequency-domain characterization of FR-4 and time-domain causality. *IEEE Transactions on Electromagnetic Compatibility*, *43*(4), 662–667. https://doi.org/10.1109/15.974647

Dobčnik, D., Gros, I., & Kolar, M. (1998). A silver/silver sulphide selective electrode prepared by means of chemical treatments of silver wire. *Acta Chimica Slovenica*, *45*(3), 209–216. Retrieved from http://acta-arhiv.chem-soc.si/45/acta1998.html

Dirkse, T. P., & Vries, D. B. de. (1959). The Effect of Continuously Changing Potential on the Silver Electrode in Alkaline Solutions. *The Journal of Physical Chemistry*, *63*(1), 107–110. https://doi.org/10.1021/j150571a028

Dutta, G., Regoutz, A., & Moschou, D. (2018). Commercially Fabricated Printed Circuit Board Sensing Electrodes for Biomarker Electrochemical Detection: The Importance of Electrode Surface Characteristics in Sensor Performance. *Proceedings*, *2*(13), 741. https://doi.org/10.3390/proceedings2130741

Ellis, H (Ed.). (1984). *Nuffield Advance Science Book of Data*. Harlow: Longman.

Ezhil Vilian, A. T., Dinesh, B., Muruganantham, R., Choe, S. R., Kang, S.-M., Huh, Y. S., & Han, Y.-K. (2017). A screen printed carbon electrode modified with an amino-functionalized metal organic framework of type MIL-101(Cr) and with palladium nanoparticles for voltammetric sensing of nitrite. *Microchimica Acta*, *184*(12), 4793–4801. https://doi.org/10.1007/s00604-017-2513-8

Ferrari, R. Ap., Pighinelli, A. L. M. T., & Park, K. J. (2011). Biodiesel Production and Quality. In M. A. D. S. Bernardes (Ed.), *Biofuel's Engineering Process Technology* (pp.221-242). https://doi.org/10.5772/17079

Fleischmann, M., Lax, D. J., & Thirsk, H. R. (1968). Electrochemical studies of the Ag2O/AgO phase change in alkaline solutions. *Transactions of the Faraday Society*, *64*(0), 3137–3146. https://doi.org/10.1039/TF9686403137

Fleischmann, M., & Pons, S. (1987). The behavior of microelectrodes. *Analytical Chemistry*, *59*(24), 1391A-1399A. https://doi.org/10.1021/ac00151a001

Fletcher, S. (2015). Screen-printed carbon electrodes. In R. C. Alkire, P. N. Bartlett, J. Lipkowski (Ed.), *Electrochemistry of Carbon Electrodes* (pp. 425-444). https://doi.org/10.1002/9783527697489.ch12

Foguel, M. v, Santos, G. P. dos, Ferreira, A. A. P., Magnani, M., Mascini, M., Skladal, P., … Yamanaka, H. (2016). Comparison of gold CD-R types as electrochemical device and as platform for biosensors. *Journal of the Brazilian Chemical Society*, *27*(4), 650–662. http://dx.doi.org/10.5935/0103-5053.20150308

Foster, R. J., & Keyes, T. E. (2006). Ultramicroelectrodes. In C. G. Zoski (Ed.), *Handbook of electrochemistry*. (pp. 155-260). Retrieved from https://search.proquest.com/docview/2130960607/8A9546F7252C4E77PQ/1?accountid=201395

Giri, S. D., & Sarkar, A. (2016). Electrochemical Study of Bulk and Monolayer Copper in Alkaline Solution. *Journal of the Electrochemical Society*, *163*(3), H252–H259. https://doi.org/10.1149/2.0071605jes

Grozdić, T. D., & Stojić, D. L. (1999). Electrochemical characteristics of binary silver alloys in alkaline solution. *Journal of Power Sources*, *79*(1), 1–8. https://doi.org/10.1016/S0378-7753(98)00160-8

Gupta, J., Juneja, S., & Bhattacharya, J. (2020). UV Lithography-Assisted Fabrication of Low-Cost Copper Electrodes Modified with Gold Nanostructures for Improved Analyte Detection. *ACS Omega*, *5*(7), 3172–3180. https://doi.org/10.1021/acsomega.9b03125

Hoar, T. P., & Dyer, C. K. (1972). The silver/silver-oxide electrode—I. Development of electrode by slow ac cycling. *Electrochimica Acta*, *17*(9), 1563–1584. https://doi.org/https://doi.org/10.1016/0013-4686(72)85048-5

Honeychurch, K. C., Hawkins, D. M., Hart, J. P., & Cowell, D. C. (2002). Voltammetric behaviour and trace determination of copper at a mercury-free screen-printed carbon electrode. *Talanta*, *57*(3), 565–574. https://doi.org/10.1016/S0039-9140(02)00060-7

Hu, C.-C., & Liu, K.-Y. (1999). Voltammetric investigation of platinum oxides. I. Effects of ageing on their formation/reduction behavior as well as catalytic activities for methanol oxidation. *Electrochimica Acta*, *44*(16), 2727–2738. https://doi.org/10.1016/S0013-4686(98)00400-9

Izutsu, K. (2002). *Electrochemistry in Nonaqueous Solutions*. https://doi.org/10.1002/3527600655

Kadara, R. O., Jenkinson, N., & Banks, C. E. (2009). Disposable Bismuth Oxide Screen Printed Electrodes for the High Throughput Screening of Heavy Metals. *Electroanalysis*, *21*(22), 2410–2414. https://doi.org/10.1002/elan.200900266

Kaye, G. W. C., & Laby, T. H.. (1986). *Tables of Physical and Chemical Constants* (l5th ed.). London: Longman.

Krejčí, J., Prášek, J., Fujcik, L., Khatib, S., Hejátková, E., Jakubka, L., & Giannoudi, L. (2004). Screen-printed sensors with graphite electrodes–comparison of properties and physical method of sensitivity enhancement. *Microelectronics International*, *21*(3), 20-24. https://doi.org/10.1108/13565360410549684

Laitinen, H. A., & Kolthoff, I. M. (1939). A study of diffusion processes by electrolysis with microelectrodes. *Journal of the American Chemical Society*, *61*(12), 3344–3349. https://doi.org/10.1021/ja01267a033

Laschi, S., Palchetti, I., & Mascini, M. (2006). Gold-based screen-printed sensor for detection of trace lead. *Sensors and Actuators B: Chemical*, *114*(1), 460–465. https://doi.org/https://doi.org/10.1016/j.snb.2005.05.028

Ledo, A., Fernandes, E., Brett, C. M. A., & Barbosa, R. M. (2020). Enhanced selectivity and stability of ruthenium purple-modified carbon fiber microelectrodes for detection of hydrogen peroxide in brain tissue. *Sensors and Actuators B: Chemical*, *311*, 127899. https://doi.org/https://doi.org/10.1016/j.snb.2020.127899

Ledru, S., Ruillé, N., & Boujtita, M. (2006). One-step screen-printed electrode modified in its bulk with HRP based on direct electron transfer for hydrogen peroxide detection in flow injection mode. *Biosensors and Bioelectronics*, *21*(8), 1591–1598. https://doi.org/https://doi.org/10.1016/j.bios.2005.07.020

Lee, J.-H., Lim, T.-S., Seo, Y., Bishop, P. L., & Papautsky, I. (2007). Needle-type dissolved oxygen microelectrode array sensors for in situ measurements. *Sensors and Actuators B: Chemical*, *128*(1), 179–185. https://doi.org/https://doi.org/10.1016/j.snb.2007.06.008

Lingane, J. J., & Lingane, P. J. (1963). Chronopotentiometry of hydrogen peroxide with a platinum wire electrode. *Journal of Electroanalytical Chemistry (1959)*, *5*(6), 411–419. https://doi.org/10.1016/0022-0728(63)80050-9

Marioli, J. M., & Sereno, L. E. (1996). Electrochemical Detection of Underivatized Amino Acids with a Ni-Cr Alloy Electrode. *Journal of Liquid Chromatography & Related Technologies*, *19*(15), 2505–2515. https://doi.org/10.1080/10826079608014033

Martins, J. I., Nunes, M. C., Koch, R., Martins, L., & Bazzaoui, M. (2007). Electrochemical oxidation of borohydride on platinum electrodes: The influence of thiourea in direct fuel cells. *Electrochimica acta*, *52*(23), 6443-6449. https://doi.org/10.1016/j.electacta.2007.04.066

Maruta, A. H., & Paixão, T. R. L. C. (2012). Flow injection analysis of free glycerol in biodiesel using a copper electrode as an amperometric detector. *Fuel*, *91*(1), 187–191. https://doi.org/https://doi.org/10.1016/j.fuel.2011.06.071

Masawat, P., & Slater, J. M. (2007). The determination of tetracycline residues in food using a disposable screen-printed gold electrode (SPGE). *Sensors and Actuators B: Chemical*, *124*(1), 127–132. https://doi.org/https://doi.org/10.1016/j.snb.2006.12.010

McGarraugh, G. (2009). The chemistry of commercial continuous glucose monitors. *Diabetes Technology & Therapeutics*, *11*(S1), S-17-S-24. http://doi.org/10.1089/dia.2008.0133

Metters, J. P., Tan, F., Kadara, R. O., & Banks, C. E. (2012). Platinum screen printed electrodes for the electroanalytical sensing of hydrazine and hydrogen peroxide. *Analytical Methods*, *4*(5), 1272–1277. https://doi.org/10.1039/C2AY05934G

Moreira, F. T. C., Ferreira, M. J. M. S., Puga, J. R. T., & Sales, M. G. F. (2016). Screen-printed electrode produced by printed-circuit board technology. Application to cancer biomarker detection by means of plastic antibody as sensing material. *Sensors and Actuators B: Chemical*, *223*, 927–935. https://doi.org/https://doi.org/10.1016/j.snb.2015.09.157

Mosquera, N., Aguirre, M. J., Ruiz-León, D., García, C., Arce, R., & Bollo, S. (2017). Co_2SnO_4/carbon paste electrode as electrochemical sensor for hydrogen peroxide. *Journal of the Chilean Chemical Society*, *62*(2), 3525–3528. https://doi.org/10.4067/S0717-97072017000200020

Muller, R. H., & Smith, C. G. (1980). Use of film-formation models for the interpretation of ellipsometer observations. *Surface Science*, *96*(1), 375–400. https://doi.org/https://doi.org/10.1016/0039-6028(80)90315-5

Neelakantan, L., & Hassel, A. W. (2007). Rotating disc electrode study of the electropolishing mechanism of NiTi in methanolic sulfuric acid. *Electrochimica Acta*, *53*(2), 915–919. https://doi.org/10.1016/j.electacta.2007.08.007

Nothdurft, P., Riess, G., & Kern, W. (2019). Copper/Epoxy Joints in Printed Circuit Boards: Manufacturing and Interfacial Failure Mechanisms. *Materials*, *12*(3), 550. https://doi.org/10.3390/ma12030550

Patrick, R.L. (1970), Interface conversion for polymer coatings. Phillip Weiss and G. Dale Cheever, editors. American elsevier publishing co., N. Y., N. Y., 1968, 389 pp. *Journal of Polymer Science Part B: Polymer Letters*, *8*(4): 309-311. https://doi.org/10.1002/pol.1970.110080421

Pissinis, D. E., Sereno, L. E., & Marioli, J. M. (2012). *Utilization of special potential scan programs for cyclic voltammetric development of different nickel oxide-hydroxide species on Ni based electrodes*. *Open Journal of Physical Chemistry*, *2*(1), 23-33. https://doi.org/10.4236/ojpc.2012.21004

Rao, C. R. K., & Trivedi, D. C. (2005). Chemical and electrochemical depositions of platinum group metals and their applications. *Coordination Chemistry Reviews*, *249*(5), 613–631. https://doi.org/10.1016/j.ccr.2004.08.015

Renedo, O. D., Alonso-Lomillo, M. A., & Martínez, M. J. A. (2007). Recent developments in the field of screen-printed electrodes and their related applications. *Talanta*, *73*(2), 202–219. https://doi.org/10.1016/j.talanta.2007.03.050

Screen-printed electrode [Image]. Retrieved May 17, 2020 from http://www.dropsens.com/en/screen_printed_electrodes_pag.html.

Serrapede, M., Pesce, G. L., Ball, R. J., & Denuault, G. (2014). Nanostructured Pd Hydride Microelectrodes: In Situ Monitoring of pH Variations in a Porous Medium. *Analytical Chemistry*, *86*(12), 5758–5765. https://doi.org/10.1021/ac500310j

Shrivastava, A., & Gupta, V. (2011). Methods for the determination of limit of detection and limit of quantitation of the analytical methods. *Chronicles of Young Scientists*, *2*(1), 21–25. https://doi.org/10.4103/2229-5186.79345

Shulga, O., & Kirchhoff, J. R. (2007). An acetylcholinesterase enzyme electrode stabilized by an electrodeposited gold nanoparticle layer. *Electrochemistry Communications*, *9*(5), 935–940. https://doi.org/https://doi.org/10.1016/j.elecom.2006.11.021

Skoog, D. A., Holler, F. J., & Crouch, S. R. (2007). *Principles of instrumental analysis* (sixth ed.). Brooks/Cole, Cengage Learning.

Smith, J. R., Campbell, S. A., & Walsh, F. C. (1995). Cyclic Voltammetry at Metal Electrodes. *Transactions of the IMF*, *73*(2), 72–78. https://doi.org/10.1080/00202967.1995.11871062

Sophocleous, M., & Atkinson, J. K. (2017). A review of screen-printed silver/silver chloride (Ag/AgCl) reference electrodes potentially suitable for environmental potentiometric sensors. *Sensors and Actuators A: Physical*, *267*, 106–120. https://doi.org/10.1016/j.sna.2017.10.013

Stonehart, P. (1968). Potentiodynamic determination of electrode kinetics for chemisorbed reactants: The $Ag/Ag_2O/OH-$ system. *Electrochimica Acta*, *13*(8), 1789–1803. https://doi.org/https://doi.org/10.1016/0013-4686(68)80087-8

Su, W.-Y., Wang, S.-M., & Cheng, S.-H. (2011). Electrochemically pretreated screen-printed carbon electrodes for the simultaneous determination of aminophenol isomers. *Journal of Electroanalytical Chemistry*, *651*(2), 166–172. https://doi.org/https://doi.org/10.1016/j.jelechem.2010.11.028

Swain, G. M. (2007). 5 - Solid Electrode Materials: Pretreatment and Activation. In C. G. Zoski (Ed.), Handbook of electrochemistry. (pp. 111-153). Retrieved from https://search.proquest.com/docview/2130960607/8A9546F7252C4E77PQ/1?accountid=201395

Taleat, Z., Khoshroo, A., & Mazloum-Ardakani, M. (2014). Screen-printed electrodes for biosensing: a review (2008-2013). *Microchimica Acta*, *18*(9-10), 865–891. https://doi.org/10.1007/s00604-014-1181-1

Tilak, B. v, Perkins, R. S., Kozlowska, H. A., & Conway, B. E. (1972). Impedance and formation characteristics of electrolytically generated silver oxides—I formation and reduction of surface oxides and the role of dissolution processes. *Electrochimica Acta*, *17*(8), 1447–1469. https://doi.org/10.1016/0013-4686(72)80088-4

Ureta-Zanartu, M. S., Montenegro, M., & Zagal, J. H. (2001). Methanol electro-oxidation on Pt-Rh alloys in acid medium. *Boletín de La Sociedad Chilena de Química*, *46*(2), 209–216. http://dx.doi.org/10.4067/S0366-16442001000200016

Villiard, F., & Jerkiewicz, G. (1997). Comprehensive studies of formation and reduction of surface oxides at rhodium electrodes at 298 K. *Canadian Journal of Chemistry*, *75*(11), 1656-1665.

Walsh, F. C. (1991). Electrode reactions in metal finishing. *Transactions of the IMF*, *69*(3), 107-110. https://doi.org/10.1080/00202967.1991.11870904

Wan, J., Wang, W., Yin, G., & Ma, X. (2012). Nonenzymatic H_2O_2 Sensor Based on Pt Nanoflower Electrode. *Journal of Cluster Science*, *23*(4), 1061–1068. https://doi.org/10.1007/s10876-012-0497-4

Wan, Y., Wang, X. L., Liu, S. Y., Li, Y., Sun, H., & Wang, Q. (2013). Effect of electrochemical factors on formation and reduction of silver oxides. *International Journal of Electrochemical Science*, *8*(12), 12837–12850. Retrieved from http://www.electrochemsci.org/list13.htm#issue12

Weinschenk, S., Mergenthaler, C., Armstrong, C., Göllner, R., Hollmann, M. W., & Strowitzki, T. (2017). Local Anesthetics, Procaine, Lidocaine, and Mepivacaine Show Vasodilatation but No Type 1 Allergy: A Double-Blind, Placebo-Controlled Study. *BioMed Research International*, *2017*, 9804693. https://doi.org/10.1155/2017/9804693

West, R. C. (Ed.). (1974). *Handbook of Chemistry and Physics* (5th ed.). Cleveland, Ohio: CRC Press/

Zhang, J. X. J., & Hoshino, K. (2013). *Molecular Sensors and Nanodevices: Principles, Designs and Applications in Biomedical Engineering*. Retrieved from https://search.proquest.com/docview/2131300074/D5643BB65198438E PQ/2?accountid=201395

Zhao, C., Shao, C., Li, M., & Jiao, K. (2007). Flow-injection analysis of glucose without enzyme based on electrocatalytic oxidation of glucose at a nickel electrode. *Talanta*, *71*(4), 1769–1773. https://doi.org/https://doi.org/10.1016/j.talanta.2006.08.013